Critical phenomena at perfect and non-perfect surfaces

2004 J. Phys. A: Math. Gen. 37 R79

(http://iopscience.iop.org/0305-4470/37/19/R01)

INSTITUTE OF PHYSICS PUBLISHING JOURNAL OF PHYSICS A: MATHEMATICAL AND GENERAL

J. Phys. A: Math. Gen. **37** (2004) R79–R115 PII: S0305-4470(04)76021-7

TOPICAL REVIEW

Critical phenomena at perfect and non-perfect surfaces

M Pleimling

Institut für Theoretische Physik I, Universität Erlangen-Nürnberg, D-91058 Erlangen, Germany

E-mail: pleim@theorie1.physik.uni-erlangen.de

Received 9 February 2004, in final form 19 March 2004
Published 27 April 2004
Online at stacks.iop.org/JPhysA/37/R79
DOI: 10.1088/0305-4470/37/19/R01

Abstract

In the past, perfect surfaces have been shown to yield local critical behaviour that differs from bulk critical behaviour. On the other hand, surface defects, whether they are of natural origin or created artificially, are known to modify local quantities. It is therefore important to clarify whether these defects are relevant or irrelevant for the surface critical behaviour.

The purpose of this review is two-fold. In the first part we summarize some of the important results on surface criticality at perfect surfaces. Special attention is thereby paid to new developments such as for example the study of the surface critical behaviour in systems with competing interactions or of surface critical dynamics. In the second part the effect of surface defects (presence of edges, steps, quenched randomness, lines of adatoms, regular geometric patterns) on local critical behaviour in semi-infinite systems and in thin films is discussed in detail. Whereas most of the defects commonly encountered are shown to be irrelevant, some notable exceptions are highlighted. It is shown furthermore that under certain circumstances non-universal local critical behaviour may be observed at surfaces.

PACS numbers: 68.35.Rh, 75.40.−s, 64.60.−i

1. Introduction

Our current understanding of critical phenomena results from an intensive interplay between experimental studies of a large variety of physical systems, ground-breaking theoretical developments (including renormalization group methods, finite-size scaling theory and conformal invariance) and extensive numerical investigations of model systems. In many cases, the systems under investigation are treated as bulk systems, thus neglecting the existence of surfaces which are unavoidable in real physical systems. Discarding surfaces in systems with short-range interactions is justifiable when studying bulk critical properties, as the contribution of the surface to extensive quantities is vanishing in the thermodynamic limit. However, a surface breaks the translation symmetry of a system and changes local quantities. Thirty years ago, it was realized that this leads to surface critical behaviour which differs from bulk critical behaviour. Since that time numerous theoretical and experimental studies have been undertaken in order to determine local critical quantities in systems with perfect surfaces.

Real surfaces, however, are usually not perfectly smooth but display some degree of roughness due to the presence of surface defects, such as for example steps, islands, or vacancies. Impurities are also often encountered at crystalline surfaces and may be viewed as the source of some disorder at the surface. Furthermore, experimentalists nowadays create thin films which do not appear in nature, by growing artificial structures on the film surface. All these defects have some impact on magnetic surface quantities.

The present work reviews the recent progress achieved in the study of critical phenomena in systems with boundaries. Besides semi-infinite systems and films with perfect surfaces, more complex geometries with wedges and corners as well as more realistic surfaces with defects are discussed. The review hereby focuses on the question whether the different types of geometries and/or of surface defects have an impact on the surface critical behaviour. It is therefore complementary to earlier reviews on surface criticality [1–4] that exclusively considered flat, perfect surfaces.

The thermodynamics of a surface is completely described by the surface free energy per area F_s. Singularities occurring in F_s determine the phase diagram of semi-infinite systems. At some phase boundaries of this phase diagram surface and bulk free energies both exhibit singularities, whereas at other boundaries only F_s becomes singular. An example for the former case is the *ordinary transition* where bulk and surface ordering occur at the same temperature, whereas the latter case is encountered at the so-called *surface transition* where the surface layer alone orders, while the bulk remains disordered. This surface transition is encountered at temperatures higher than the bulk critical temperature, the critical fluctuations of the d-dimensional semi-infinite system then being essentially $(d-1)$-dimensional, corresponding to a phase transition in $d-1$ dimensions.

In section 2, the critical behaviour at perfect surfaces is discussed. At the bulk critical point different surface universality classes are obtained for every bulk universality class. These universality classes are discussed and their differences emphasized. Furthermore, recent progress in our understanding of the surface critical behaviour in systems with competing interactions is reviewed. Surface critical dynamics and the effect of symmetry breaking surface fields are also briefly discussed. Section 3 is devoted to more complex geometries with a wedge. Wedge-shaped models are very interesting systems where local critical exponents, which change continuously with the wedge opening angle, arise because of the particular geometrical properties of the wedge. However, at a given opening angle, the surface critical behaviour for the ordinary transition is still universal and does not depend on microscopic details of the model, such as for example the lattice type or the strengths of the local interactions. This is completely different from that for the surface transition, where under certain circumstances non-universal local critical behaviour can be observed. At a fixed opening angle, edge critical exponents then not only depend continuously on the values of the local couplings but also reflect the existence of the disordered bulk. This intriguing behaviour results from the fact that at the surface transition the edge acts like a defect line in a two-dimensional critical system. Corner critical behaviour is discussed in this section, too. In the last few years, a great deal of activity focused on the critical behaviour of wedges in the presence of external surface fields. This rapidly developing field is also briefly summarized.

Section 4 deals with the important issue of thin films and semi-infinite systems with non-perfect surfaces. Surfaces are very often naturally rough, due to the growth mechanism or because of erosion effects. Adatom islands, vacancy islands or steps are typical defects encountered at real surfaces. On the other hand, specific surface structures, such as for example lines of adatoms or regular geometrical patterns, can be created on purpose by using advanced experimental methods. As these surface defects have an impact on local surface quantities, one has to ask the question whether they change the surface critical behaviour. For semi-infinite systems, we must again distinguish between the ordinary transition and the surface transition. For the ordinary transition, common surface defects (presence of a step, surfaces with uncorrelated roughness, amorphous surface) are usually irrelevant for the surface critical behaviour, but there are some notable exceptions. For the surface transition, defect structures such as steps and additional lines of atoms located at the surface may yield non-universal local critical exponents, as observed in semi-infinite Ising models with additional surface structures. Interestingly, additional lines located at the surface of thin Ising films always lead to non-universal local critical behaviour. Section 5 finally contains concluding remarks.

2. Perfect surfaces

The aim of this section is to review the main results on surface criticality in systems with flat, perfect surfaces. In sections 2.1 and 2.2, we pay special attention to the phase diagrams of semi-infinite systems as well as to the sets of critical exponents characterizing the different surface phase transitions. As the number of papers published on this topic is rather impressive, only selected results are presented. The interested reader is referred to the reviews of Binder [1], Abraham [2] and Diehl [3, 4] for further reading. The main experimental techniques available for the investigation of surface critical behaviour are reviewed in the book of Dosch [5]. Section 2.3 is devoted to critical phenomena in thin films, whereas in section 2.4 the recent studies of the surface criticality in systems with competing interactions are discussed. Brief accounts of works on surface critical dynamics and on surface critical behaviour in the presence of external fields close this section.

2.1. Surface quantities and phase diagrams

When comparing systems with and without surfaces, one remarks that extensive quantities are altered by the presence of surfaces. Thus, the free energy is given by [6, 7]

$$F = F_b V + F_s S + \cdots \tag{1}$$

with the bulk free energy per volume F_b and the surface free energy per surface area F_s. V and S are the volume and the surface of the system, respectively. Further terms in equation (1) may result from the presence of edges, as discussed in section 3. Similar corrections also show up in other extensive quantities.

The surface free energy F_s completely describes the thermodynamics of the surface. Similar to F_b, singularities occur in F_s. The values of the variables of F_s, where these singularities appear, determine the boundaries separating the different phases of the surface phase diagram. As we shall see later in the course of this section, at some phase boundaries both F_b and F_s exhibit singularities whereas at others only F_s becomes singular.

Local quantities such as the local magnetization density (often called local magnetization for brevity) or the local energy density are also modified by the presence of a surface. Examples of order parameter profiles obtained by Monte Carlo simulations of three-dimensional Ising films with $L = 80$ layers at temperatures below the bulk critical temperature $k_B T_c / J_b = 4.5115$

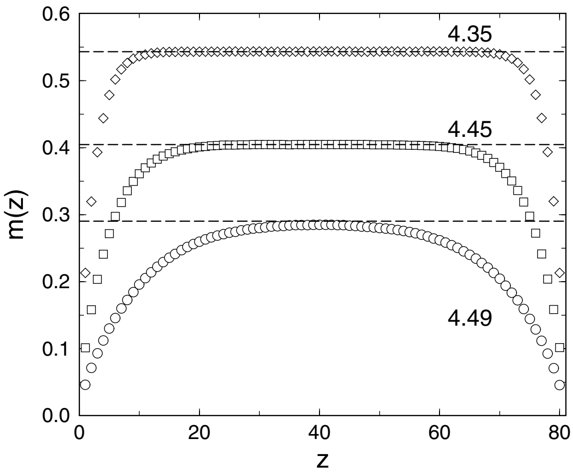

Figure 1. Order parameter profiles $m(z)$ of a three-dimensional Ising film with 80 layers at three different temperatures $k_B T/J_b$. The dashed lines denote the bulk values ([8]).

are shown in figure 1 [8]. Here, all the couplings involved have been chosen to have equal strength J_b and no magnetic fields have been retained. The surface magnetization $m_1 = m(1) = m(L)$, related to F_s by the equation

$$m_1 = -\frac{\partial F_s}{\partial H_1} \tag{2}$$

is smaller than the bulk magnetization due to the reduced coordination number at the surface. The field H_1 acts exclusively on the surface layer. The magnetization increases from its surface value to the bulk value at distances exceeding the bulk correlation length ξ_b. In the case that, the thickness of the film is not large compared to ξ_b (such as for example at the temperature $k_B T/J_b = 4.49$ in figure 1) the bulk magnetization is never reached. For surface couplings exceeding the bulk couplings by a large amount, magnetization profiles decreasing monotonically towards the centre of the system may also be observed.

For Ising models in film geometry we have the general Hamiltonian

$$\mathcal{H} = -J_b \sum_{\langle ij \rangle} s_i s_j - J_s \sum_{\substack{\langle ij \rangle \\ \text{surface}}} s_i s_j - H \sum_i s_i - H_1 \sum_{\text{surface}} s_i \tag{3}$$

where the spins s_i can take on the values ± 1. The first sum runs over bonds connecting neighbouring spins where at least one of the spins is a bulk spin, whereas the second sum runs over all surface links. Bulk couplings, J_b, and surface couplings, J_s, are ferromagnetic. The bulk field H acts on all the spins, the surface field H_1 only on spins located at the surface, i.e. a surface spin sees the field $H + H_1$. Sometimes a different coupling constant is used for the bonds connecting surface and bulk spins [9]. In general, the perturbations due to the presence of a surface are supposed to be of short range.

Analytical results on the surface critical behaviour are commonly obtained in the framework of continuum field theory, see [3, 4] for comprehensive reviews. The standard ϕ^4 Ginzburg–Landau model, appropriate for the universality class of the Ising model, is thereby augmented in order to include contributions coming from the surface:

$$f_s := F_s/k_B T = \tfrac{1}{2} c_0 \phi^2 - h_1 \phi \tag{4}$$

Table 1. Surface critical exponents and their definitions.

Surface exponent	Definition
β_1	$m_1 \sim t^{\beta_1}$
γ_1	$\chi_1 \sim \lvert t\rvert^{-\gamma_1}$
γ_{11}	$\chi_{11} \sim \lvert t\rvert^{-\gamma_{11}}$
β_s	$m_s \sim t^{\beta_s}$
γ_s	$\chi_s \sim \lvert t\rvert^{-\gamma_s}$
α_s	$C_s \sim \lvert t\rvert^{-\alpha_s}$
x_1	$G_{\mathrm{par}}(\vec{\rho} - \vec{\rho}') \sim \lvert\vec{\rho} - \vec{\rho}'\rvert^{-2x_1}$
Φ	$\lvert T_s(c) - T_{\mathrm{c}}\rvert / T_{\mathrm{c}} \sim \lvert c\rvert^{1/\Phi}$

with $h_1 := H_1/k_B T$, whereas c_0 is related to the surface enhancement of the spin–spin coupling constant in the corresponding lattice model. The resulting Ginzburg–Landau free energy density is readily generalized to cases where the order parameter exhibits a different symmetry.

Layer-dependent quantities are very useful when investigating systems with surfaces. Examples are the magnetization per layer $m(z)$ and the susceptibility per layer $\chi(z)$ where z labels the layers parallel to the surface. The surface magnetization is $m_1 = m(z = 1)$ and the local susceptibility at the surface, i.e. the response of the surface magnetization to a surface field, $\chi_{11} = -\frac{\partial^2 F_s}{\partial H_1^2}$, is given by $\chi_{11} = \chi(z = 1)$. From the profiles $m(z)$ and $\chi(z)$ one also obtains the surface excess quantities

$$m_s = -\frac{\partial F_s}{\partial H} = \sum_{z=1} (m(z) - m_b) \tag{5}$$

and

$$\chi_s = -\frac{\partial^2 F_s}{\partial H^2} = \sum_{z=1} (\chi(z) - \chi_b) \tag{6}$$

where m_b and χ_b are the bulk magnetization and the bulk susceptibility. Of further importance is the surface layer susceptibility, i.e. the response of the local surface magnetization to a bulk field, usually denoted by χ_1. The critical surface pair correlation function behaves as

$$G_{\mathrm{par}}(\vec{\rho} - \vec{\rho}') \sim |\vec{\rho} - \vec{\rho}'|^{-2x_1} \tag{7}$$

where x_1 is the scaling dimension of the surface order parameter. For a d-dimensional model $\vec{\rho}$ is a $(d-1)$-dimensional vector parallel to the surface. This behaviour of the surface correlation function differs from that of the bulk correlation function:

$$G_b(\vec{r} - \vec{r}') \sim |\vec{r} - \vec{r}'|^{-2x_b} \tag{8}$$

where the value of the bulk scaling dimension x_b is usually smaller than that of x_1. Here $\vec{r}$ is a d-dimensional vector. Critical correlations between a surface point and a bulk point exhibit a power-law behaviour with the exponent $x_1 + x_b$. The surface critical exponents associated with the different critical quantities are listed in table 1.

The phase diagram of the three-dimensional semi-infinite Ising model is well established. The global phase diagram of the semi-infinite system depends not only on the values of the coupling constants and on the temperature but also on the external fields H and H_1 [10]. I discuss in the following only the case of vanishing external fields. The qualitative results obtained in the mean-field approximation [1, 9, 11–13] represent the correct phase diagram as derived from renormalization group calculations [14, 15] and from Monte Carlo simulations

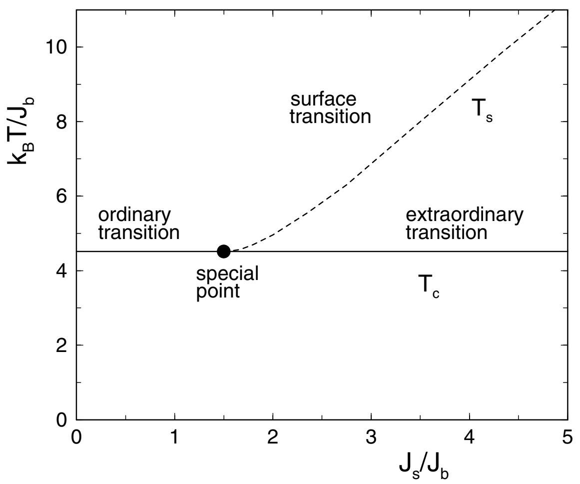

Figure 2. Surface phase diagram of the semi-infinite three-dimensional Ising model.

[13, 16] quite well, see figure 2. If the ratio of the surface coupling J_s to the bulk coupling J_b, $r = J_s/J_b$, is sufficiently small, the system undergoes at the bulk critical temperature T_c an ordinary transition, with the bulk and surface ordering occurring at the same temperature. Beyond a critical ratio, $r > r_{sp} \approx 1.50$ for the semi-infinite Ising model on the simple cubic lattice [16–18], the surface orders at the so-called surface transition at a temperature $T_s > T_c$, followed by the extraordinary transition of the bulk at T_c. At the critical ratio r_{sp}, one encounters the multicritical special transition point, with critical surface properties deviating from those at the ordinary transition and those at the surface transition. In the mean-field approximation, the critical ratio at the special transition point is $r_{sp}^{MF} = 1.25$ for the simple cubic lattice.

In the field theoretical formulation of the problem, see equation (4), three stable renormalization-group fixed-point values for c_0 can be shown to exist in the absence of external fields. For $c_0 = +\infty$, resp. $c_0 = -\infty$, one is dealing with the critical behaviour of the ordinary, resp. extraordinary, transition. The fixed point corresponding to the special transition is located at $c_0 = c_{SP}$. Usually, a new variable $c \sim c_0 - c_{SP}$ is introduced, such that the ordinary transition occurs for $c > 0$, whereas the extraordinary transition is observed for supercritical enhancements $c < 0$, the special transition point then being located at $c = 0$.

The mean-field approximation yields similar surface phase diagrams for all $O(n)$ models in all dimensions. Of course, this scenario with three lines of continuous phase transitions is only realized in systems where the surface can sustain long-range order, independently of the bulk. Rigorous results [19] show that only the ordinary transition is encountered in the two-dimensional Ising model with short-range interactions in the absence of external fields. This is readily understood as the surface is then one dimensional. For continuous spins with $n \geqslant 3$ and isotropic couplings, a surface transition, where only the surface orders, does not exist in three dimensions, in accordance with the well-known Mermin–Wagner theorem [20]. Indeed, the surface effectively decouples from the bulk for very strong surface couplings $J_s \gg J_b$ and then forms an isolated two-dimensional system. An interesting case is that of the XY ($n = 2$) model which has a Kosterlitz–Thouless transition in two dimensions [21, 22]. A phase diagram similar to figure 2 has been shown to exist for the three-dimensional semi-infinite XY model [23–25] with the surface undergoing a Kosterlitz–Thouless transition for coupling ratios larger then some critical value, the bulk remaining disordered. Due to the peculiar properties of this transition, the multicritical special transition point is then of a special nature. Diehl and Eisenriegler have shown that in semi-infinite $O(n)$ models (and therefore also in the experimental relevant case of the semi-infinite Heisenberg model in three dimensions) anisotropic surface couplings may lead to an anisotropic special transition point and to a surface transition where the bulk remains disordered [26]. Phase diagrams similar to figure 2 are found for all $O(n)$ models with isotropic couplings above the upper critical dimension.

The models mentioned so far only cover a fraction of the research on surface critical phenomena. Other semi-infinite models studied include, for example, spin-1 Ising models [27], Blume–Emery–Griffiths models [28], Potts models [29], ferrimagnetic Ising models [30], layered magnetic systems [31] or bond percolation in the semi-infinite system (which can be regarded as the ($q \longrightarrow 1$)-limit of the q-state Potts model) [32–36].

Before discussing the various surface universality classes, I want to mention two further interesting cases. For systems with a discontinuous phase transition, the surface order parameter may change continuously as the bulk transition point is approached. As discussed by Lipowsky [37] (see also [38]) universal surface properties may show up for this case too. In the presence of this so-called surface-induced disorder, correlation lengths both parallel and perpendicular to the surface diverge at the bulk first-order transition point, thus inducing anisotropic power-law behaviour for some bulk quantities [39]. A possible realization of this scenario may be encountered in the antiferromagnet UO_2 where the surface layers order continuously while the bulk displays a discontinuous ordering [40]. A second intriguing scenario is encountered in the q-state Potts model [41, 42] where a phase transition to a low-temperature phase with an ordered bulk but a disordered surface is observed.

2.2. The surface universality classes

It is obvious from the preceding discussion of possible surface phase diagrams that for every bulk universality class different surface universality classes may be realized. The different surface universality classes will be discussed in the following in more detail and their differences emphasized.

At the ordinary transition both bulk and surface order at the bulk critical temperature. The ordinary transition is the only phase transition which is observed in the surface phase diagrams of all ferromagnetic three-dimensional $O(n)$ models in the absence of symmetry-breaking fields. It has been studied intensively, both by analytical and by numerical methods. The surface critical exponents at the ordinary transition can all be obtained by combining bulk exponents with one additional surface exponent Δ_1 [12, 13]. This new exponent results from the scaling function of the singular part of the surface free energy

$$f_s^{(\text{sing})} = |t|^{2-\alpha_s} g(|t|^{-\Delta_b} h, |t|^{-\Delta_1} \tilde{h}_1) \tag{9}$$

where $t = (T_c - T)/T_c$ is the reduced temperature and $\tilde{h}_1$ is the surface scaling field which depends on both bulk and surface fields. The bulk exponent Δ_b is known from the singular part of the bulk free energy, whereas α_s is the critical exponent of the excess specific heat C_s. Various scaling relations connect surface and bulk exponents. The critical exponents of excess quantities are obtained by combining bulk exponents:

$$\beta_s = \beta_b - \nu_b \tag{10}$$

$$\gamma_s = \gamma_b + \nu_b \tag{11}$$

$$\alpha_s = \alpha_b - \nu_b. \tag{12}$$

Table 2. Estimates of Ising surface critical exponents in three dimensions at the ordinary transition, as obtained by different techniques. MF: mean-field theory, MC: Monte Carlo techniques, FT: field-theoretical methods.

	β_1	γ_1	γ_{11}
MF [12]	1	1/2	− 1/2
MC [47]	0.78(2)	0.78(6)	
MC [48]	0.807(4)	0.760(4)	
MC [8]	0.80(1)	0.78(5)	−0.25(10)
FT [56]	0.816	0.767	−0.336
FT [44]	0.796	0.769	−0.333

Other useful scaling relations are (d being the number of space dimensions)

$$\gamma_s = 2\gamma_1 - \gamma_{11} \tag{13}$$

$$\gamma_{11} = \nu_b(d - 1 - 2x_1) \tag{14}$$

$$\gamma_1 = \nu_b(d - x_1 - x_b) \tag{15}$$

$$\beta_1 = \nu_b x_1. \tag{16}$$

Further scaling relations are discussed in [1, 3, 13].

In table 2 estimates of various three-dimensional Ising surface critical exponents obtained by different techniques are compiled. One observes a very good agreement between the recent massive field-theoretical estimates [43, 44] and the numerical estimates. Similar agreement is also obtained for other $O(n)$ models. From the numerical point of view, the best investigated cases are $n = 0$ [45, 46] and $n = 1$ (Ising) [8, 17, 18, 47, 48], whereas studies for $n \geqslant 2$ are scarce [24, 49–51]. The rather few experimental determinations of surface critical exponents at the ordinary transition, using for example x-ray scattering at grazing angle, yield values which are found to be compatible with the theoretical estimates [52–55].

Exact results can by obtained by applying conformal invariance to semi-infinite systems. As shown by Cardy [57] conformal invariance yields in two-dimensional systems the exact values of the surface critical exponents at the ordinary transition and completely fixes the correlation functions. In higher dimensions, it constrains the form of correlation functions near the free surface. Recent applications of conformal invariance include the determination of order parameter profiles in various two-dimensional systems with boundaries [58] or the computation of three-dimensional Ising surface critical exponents from models defined on half spherocylinders [59].

The special transition point, located at the coupling ratio r_{sp}, is a multicritical point where the bulk *and* the surface become critical. Three different critical lines (ordinary transition, surface transition, extraordinary transition) merge at this point. The surface criticality is thereby characterized by two new surface exponents: Δ_1^{sp} and Φ. The appropriate scaling ansatz for the singular part of the surface free energy then reads

$$f_s^{(\mathrm{sing})} = |t|^{2-\alpha_s} g_{sp}\left(|t|^{-\Delta_b} h, |t|^{-\Delta_1^{sp}} h_1, |t|^{-\Phi} c\right) \tag{17}$$

with the surface enhancement $c \sim r - r_{sp}$. The crossover exponent Φ governs the behaviour of the surface transition line close to the special transition point:

$$|T_s(c) - T_\mathrm{c}|/T_\mathrm{c} \sim |c|^{1/\Phi}. \tag{18}$$

Estimates for various surface critical exponents obtained at the special transition point of the three-dimensional semi-infinite Ising model are gathered in table 3. Again, good agreement

Table 3. Estimates of Ising surface critical exponents at the special transition point in three dimensions, as obtained by different techniques. MF: mean-field theory, MC: Monte Carlo techniques, FT: field-theoretical methods.

	β_1^{sp}	γ_1^{sp}	γ_{11}^{sp}	Φ
MF [1]	1/2	1	1/2	1/2
MC [47]	0.18(2)	1.41(14)	0.96(9)	0.59(4)
MC [18]	0.237(5)			0.461(15)
MC [48]	0.2375(15)	1.328(1)	0.788(1)	
FT [60]	0.245	1.43	0.85	0.68
FT [44]	0.263	1.302	0.734	0.539

between analytical and numerical estimates has been achieved. One also notes that the scaling laws (14)–(16) hold at this multicritical point.

For the surface enhancements exceeding the critical value r_{sp} two distinct phase transitions are encountered. The surface transition line, which is located at higher temperatures, separates the disordered high-temperature phase from a phase where the surface alone is ordered. The bulk orders at the lower bulk critical temperature in the presence of an already ordered surface. This latter transition is coined an extraordinary transition. The possible existence of a magnetic surface transition at temperatures higher than the bulk critical temperature has been suggested to exist for various compounds, such as for example Gd [61–64], Tb [65, 66], $FeNi_3$ [67], NiO [68, 69], $NbSe_2$ [70] or Ni–Al alloys [71]. However, the experimental situation is usually not very clear. A good example for the encountered experimental difficulties is Gd. Whereas it was believed for many years that Gd undergoes a transition to a surface-ordered, bulk-disordered phase some 80 °C above the bulk critical temperature, a recent study [72] claims that for pure Gd surface and bulk order at the *same* temperature, thus giving rise to ordinary transition behaviour.

Usually, the surface transition is considered to be of minor theoretical interest. This is due to the fact that at the surface transition, the surface critical behaviour of a d-dimensional semi-infinite system is expected to be identical to that of the corresponding $(d - 1)$-dimensional bulk system. Indeed, for perfect surfaces, the critical exponents of the two-dimensional bulk Ising model are encountered at the surface transition of the three-dimensional semi-infinite Ising model. However, the situation is not so simple for non-perfect surfaces presenting edges or extended surface defects. As will be discussed in detail in sections 3 and 4, the local critical behaviour at non-perfect surfaces may be non-universal at the surface transition. In that case, local critical exponents which vary continuously as a function of the local couplings are encountered. Furthermore, the presence of the disordered bulk is reflected by the values of the local critical exponents. It is worth noting that these effects are not restricted to the Ising model but are also encountered in the three-dimensional easy-axis anisotropic Heisenberg model whose surface transition belongs to the universality class of the two-dimensional Ising model.

At the extraordinary transition, the bulk orders in the presence of an ordered surface. The extraordinary transition with enhanced surface couplings and vanishing surface field is equivalent to the normal transition where the bulk orders in the presence of a field acting on the surface. This was conjectured by Bray and Moore [73] and later proved by Burkhardt and Diehl for the Ising model [74]. The normal transition occurs in confined binary liquid mixtures at their bulk critical point. The equivalence of these two transitions is very useful for experimental studies as surface ordering fields are commonly encountered whereas physical systems with a genuine extraordinary transition are very scarce. To my knowledge, the extraordinary transition has only been investigated experimentally for NiO [68, 69]. It should also be noted that some model systems possess a normal transition without exhibiting an extraordinary transition. A good example is the two-dimensional semi-infinite Ising model with short-range interactions.

Surface critical exponents at the extraordinary transition can be completely expressed by bulk exponents. The singular part of the surface magnetization, for example, varies close to the bulk critical temperature as $m_1^{(\mathrm{sing})} \sim |T - T_c|^{2-\alpha_b}$.

To conclude this section, let us finally mention the interesting possibility that the surface critical behaviour depends on the surface orientation. Examples where this dependence has been proved are binary alloys with a continuous phase transition [75] and Ising antiferromagnets in the presence of a magnetic field [75, 76]. Ordinary transition behaviour is encountered in these systems for symmetry-preserving surface orientations, whereas symmetry-breaking orientations lead to normal critical behaviour.

2.3. Thin films

Thin film magnetism is the subject of intensive current research activities, see [77] for a recent review. For the investigation of magnetic properties of thin films experimentalists have a large variety of experimental techniques at their disposal, ranging from ferromagnetic resonance to magneto-optic Kerr effect measurements. This has led to a large number of interesting results concerning the magnetism of thin films.

Critical phenomena in thin films have also been studied in recent years. In the following, I discuss some of the more general aspects of thin film critical behaviour, focusing thereby on thin films with perfect surfaces. The critical behaviour of more realistic films will be discussed in section 4.2.

First one has to remark that the critical temperature in thin films is a function of the number of layers forming the film. The temperature shift has been observed in numerous experimental studies and it has also been investigated extensively in theory [78–82]. For thick films with L layers, the deviation from the bulk critical temperature $T_c(\infty)$ is described by the well-known finite-size scaling relation [83]

$$1 - T_c(L)/T_c(\infty) \propto L^{-\lambda}. \tag{19}$$

The shift exponent λ is given by $\lambda = 1/\nu_b$ where ν_b is the correlation length critical exponent of the infinite system. In the ultrathin film limit, linear dependence of $T_c(L)/T_c(\infty)$ on the film thickness is observed, see [81] for a recent discussion.

While analysing critical quantities in films with varying thicknesses, a dimensional crossover from three-dimensional criticality for thicker films to two-dimensional critical behaviour for ultrathin films is observed [84–87], due to the truncation of the correlation length normal to the film [88]. This crossover has been studied numerically in Ising films by analysing the critical exponent of the total film magnetization [89]. Note that from a puristic point of view, the two-dimensional critical exponents should be observed for every finite film in a small-temperature range near the critical point. However, as the width of this temperature window decreases rapidly for increasing film thickness, this temperature range may not be easily accessible in experiments or in computer simulations. Recent studies investigated this crossover in various systems using local effective critical exponents [90–92].

In thicker films of some systems, a crossover from three-dimensional Heisenberg to three-dimensional Ising behaviour may be observed [87]. The formation of an easy-magnetization axis is due to an increase in the magnetic anisotropy energy. In fact, the reduced symmetry at surfaces increases the anisotropy energy as compared to bulk systems where it usually is small. A change of the direction of the easy axis is often observed when changing the thickness of the film. For example, for Ni/Cu(001) the easy axis is in-plane for ultrathin films, but an out-of-plane easy axis is observed for films with more than seven monolayers [93]. Long-range dipolar interactions contributing to the anisotropy are responsible for this behaviour. A further contribution to the magnetic anisotropy energy has its origin in the fact that (ultra)thin magnetic films are grown on a substrate. Indeed, a distortion of the lattice due to strain between the magnetic layers and the substrate may change the magnetic anisotropy energy as compared to the bulk system. The magnetic anisotropy energy is the subject of numerous theoretical studies, using different analytic methods [94] or *ab initio* techniques [95]. In a statistical treatment of surface phenomena, the change in the magnetic anisotropic energy due to the presence of surfaces is usually modelled by effective short-range couplings with varying coupling constants, see [78] for an example. Furthermore, when studying thin film critical behaviour theoretically, films are usually supposed to be free standing.

Most thin films may be grouped into two different universality classes with respect to their critical behaviour. Films with an out-of-plane easy axis are theoretically described by Ising models (e.g. the Fe/Ag(100) system [96]), whereas films with easy-plane magnetization are modelled by XY-models (e.g. the Ni/Cu(100) system [97]). Interestingly, a given material may exhibit both types of magnetization, depending on the orientation of the film and the nature of the substrate. For example, Ni(001) grown on Cu(001) presents an out-of-plane easy axis, whereas for Ni(111) on Re(0001) the magnetization is in-plane. Spin reorientation transitions as a function of surface and bulk anisotropies have been studied theoretically for thin ferromagnetic films as well as for semi-infinite ferromagnetic systems in [98].

2.4. Surface critical behaviour near a Lifshitz point

Competing interactions are encountered in a large variety of physical systems such as, among others, magnetic systems, alloys or ferroelectrics [99–103]. These interactions may lead to rich phase diagrams with a multitude of commensurately and incommensurately modulated phases as well as to special multicritical points called Lifshitz points. At a Lifshitz point, a disordered, a uniformly ordered and a periodically ordered phase become indistinguishable [104]. A large number of systems (such as, e.g., magnets, ferroelectric liquid crystals, uniaxial ferroelectrics or block copolymers) have been shown to possess a Lifshitz point.

From a theoretical point of view the best studied Lifshitz point is that encountered in the three-dimensional ANNNI model [100, 101, 105]. The Hamiltonian of this model, defined on a simple cubic lattice, reads

$$\mathcal{H} = -J \sum_{xyz} S_{xyz}(S_{(x+1)yz} + S_{x(y+1)z}) - J \sum_{xyz} S_{xyz} S_{xy(z+1)} + \kappa J \sum_{xyz} S_{xyz} S_{xy(z+2)} \tag{20}$$

with $S_{xyz} = \pm 1$. Here $J > 0$ and $\kappa > 0$ are coupling constants. In the planes nearest neighbour spins are coupled ferromagnetically with the coupling constant J, whereas in z- or axial-direction competition between ferromagnetic nearest neighbour and antiferromagnetic next-nearest neighbour couplings takes place, leading to the appearance of spatially modulated phases. In the infinite system infinitely many commensurately and incommensurately modulated phases appear in the (T, κ) phase diagram [100, 106, 107]. In thin ANNNI films, however, only modulated phases compatible with the thickness of the film may be stabilized, leading to a different phase diagram for every film thickness [108–110]. Note that the related phase transitions in thin helimagnetic and incommensurately modulated films have also been the subject of recent studies [111, 112].

The Lifshitz point encountered in the three-dimensional ANNNI model is of the uniaxial Ising type, the order parameter at this multicritical point having only one component. The

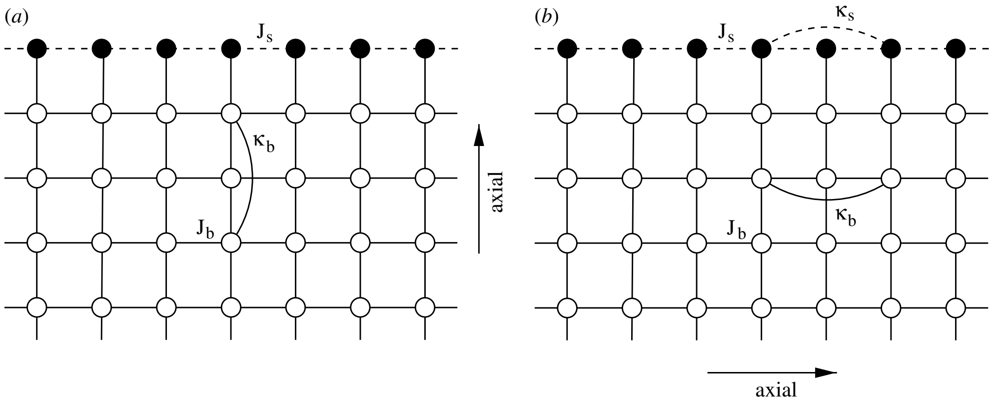

Figure 3. Cross sections of semi-infinite three-dimensional ANNNI models showing two different types of surface orientations: (*a*) surfaces perpendicular to the axis of competing interactions, (*b*) surfaces parallel to this axis. J_b and J_s denote the nearest neighbour bulk and surface couplings, respectively, whereas the axial next-nearest neighbour interactions are labelled by the bulk, κ_b, and surface, κ_s, competing parameters. Surface lattice sites are represented by filled points.

term uniaxial denotes the fact that wave vector instabilities only show up in a single direction. In general, the Ginzburg–Landau free energy density in d dimensions may be written in the presence of a uniaxial Lifshitz point in the following form:

$$f = a_2\phi^2 + a_4\phi^4 + b_1|\nabla_1\phi|^2 + b_2|\nabla_{(d-1)}\phi|^2 + c_1\left|\nabla_1^2\phi\right|^2 \tag{21}$$

where ϕ is the order parameter, ∇_1 the space derivative in the axial direction, whereas $\nabla_{(d-1)}$ is the gradient operator in the directions perpendicular to that direction. The coefficient b_1 in equation (21) may change sign because of the competition between ferro- and antiferromagnetic interactions along the special direction. At the Lifshitz point, b_1 vanishes and the last term in equation (21) becomes relevant.

A uniaxial Lifshitz point is only a special case of more general Lifshitz points [104] (see [113] for a recent brief review) characterized by the number of space dimensions, d, the number of order parameter components, n, and the dimensionality m of the subspace where the wave vector instability occurs. The Lifshitz point encountered in the three-dimensional ANNNI model is then given by the set $(d, n, m) = (3, 1, 1)$. Uniaxial Lifshitz points are strong anisotropic equilibrium critical points where the correlation lengths parallel and perpendicular to the axial axis diverge with different critical exponents $\nu_\parallel^L$ and $\nu_\perp^L$. The discovery of this kind of multicritical point in 1975 led to numerous theoretical studies of their bulk critical properties. With the exception of an early attempt by Gumbs [114], surface critical phenomena at a bulk Lifshitz point have only been studied very recently [115–120]. Most of the results have been obtained for the semi-infinite ANNNI model.

Due to the anisotropy of the ANNNI model, surfaces with different orientations are not equivalent. The following two surface orientations have been considered (see figure 3): surfaces perpendicular to the axis of competing interactions (case A) and surfaces parallel to this axis (case B). As usual, the index b (s) indicates bulk (surface) couplings in the following.

For case A modified surface couplings connecting neighbouring surface spins are introduced in addition to the usual ANNNI interactions, see figure 3(*a*). Three different scenarios have to be distinguished, depending on the value of the bulk competing parameter κ_b. When κ_b is smaller than the Lifshitz point value $\kappa_b^L = 0.27$, the bulk undergoes a second-order phase transition between the disordered high-temperature phase and the ordered, ferromagnetic, low-temperature phase at the critical temperature $T_c(\kappa_b)$. This phase transition belongs to the universality class of the three-dimensional Ising model. Consequently, the surface phase diagram will resemble that of the three-dimensional semi-infinite Ising model. At the bulk Lifshitz point, $\kappa_b = \kappa_b^L$, the recent mean-field treatment [115] yields for the semi-infinite ANNNI model a surface phase diagram similar to the Ising model, but with a set of critical exponents different from those of the Ising model. The predicted existence at the bulk Lifshitz point [115] of a special transition point is in variance with the earlier treatment of [114] but agrees with the Monte Carlo results of [118]. Finally, for axial next-nearest neighbour bulk couplings $\kappa_b > \kappa_b^L$ the bulk phase transition from the disordered to the modulated phase belongs to the universality class of the three-dimensional XY model [121]. It may then be argued that at the ordinary transition one is dealing with a critical semi-infinite three-dimensional XY model with Ising-like surface exchange anisotropies. Surface exchange anisotropies being irrelevant near the ordinary transition [26], one therefore expects the ordinary transition critical behaviour of the semi-infinite three-dimensional ANNNI model with $\kappa_b > \kappa_b^L$ to be identical to that of the three-dimensional semi-infinite XY model [24]. A surface transition belonging to the three-dimensional Ising universality class will again be encountered for strong surface enhancements. The ordinary transition and the surface transition lines are then expected to meet at an anisotropic special transition point [26].

Case B consists of surfaces oriented parallel to the axial direction (see figure 3(*b*)). The introduction of modified nearest neighbour, J_s, *and* axial next-nearest neighbour couplings, $\kappa_s > 0$, in the surface layer leads to intriguing and very complex situations. First, one has to note that the critical value of the coupling ratio r_{sp}, needed for the surface to get critical by itself, depends both on the bulk, κ_b, and on the surface, κ_s, competing parameters. Three different cases may be distinguished, depending on the value of $r = J_s/J_b$.

(1) For $r < r_{sp}(\kappa_b, \kappa_s)$ the ordinary surface transition is encountered, with Ising bulk ordering $\left(\kappa_b < \kappa_b^L\right)$, Lifshitz point bulk ordering $\left(\kappa_b = \kappa_b^L\right)$, or modulated bulk ordering $\left(\kappa_b > \kappa_b^L\right)$.

(2) For $r > r_{sp}(\kappa_b, \kappa_s)$ the surface orders at a higher temperature than the bulk. For $\kappa_s < 1/2$ the surface transition belongs to the universality class of the two-dimensional Ising model, whereas for $\kappa_s > 1/2$ a floating incommensurate phase appears in the surface layer. No surface transition, where the surface alone orders, will be encountered for $\kappa_s = 1/2$, as in the two-dimensional ANNNI model the paramagnetic phase extends down to $T = 0$ for this value of κ_s [100].

(3) For $r = r_{sp}(\kappa_b, \kappa_s)$ the special surface transition point is encountered where the ordinary transition line and the surface transition line merge. Depending on the values of κ_b and κ_s, very interesting possibilities arise. Whereas for $\kappa_b < \kappa_b^L$ and $\kappa_s < 1/2$ the usual scenario of an Ising ordinary transition meeting an Ising surface transition is encountered, for $\kappa_b = \kappa_b^L$ and $\kappa_s < 1/2$ a Lifshitz point ordinary transition merges with an Ising surface transition. These are the only cases studied so far in some detail [116, 118]. However, more exotic multicritical points may also be encountered. For example, one may have the case that at the special transition point an ordinary transition line with a modulated bulk $\left(\kappa_b > \kappa_b^L\right)$ meets a surface transition line to a floating incommensurate phase in the surface layer ($\kappa_s > 1/2$). Finally, I should also mention the rather academic possibility that in four dimensions a Lifshitz point ordinary transition $\left(\kappa_b = \kappa_b^L\right)$ merges with a Lifshitz point surface transition $\left(\kappa_s = \kappa_s^L\right)$.

In their mean-field treatment Binder, Frisch and Kimball [115, 116] considered surfaces oriented either perpendicular [115] or parallel [116] to the axis of competing interactions. For both cases the mean-field surface critical exponents at the Lifshitz point were determined

Table 4. Surface critical exponents at a uniaxial bulk Lifshitz point with the surface layer oriented perpendicular (case A) and parallel (case B) to the axial direction. OT: ordinary transition, SP: special transition point, MF: mean-field theory, MC: Monte Carlo simulations, RNG: renormalization group methods.

		β_1^L	γ_1^L	γ_{11}^L	β_s^L	γ_s^L
Case A	OT/MF [115]	1	1/2	−1/4	1/4	5/4
	OT/MC [118]	0.62(1)	0.84(5)	−0.06(2)	−0.14(4)	1.69(7)
	SP/MC [118]	0.22(2)	1.28(8)	0.76(5)		
Case B	OT/MF [116]	1	1/2	−1/2	0	3/2
	OT/MC [118]	0.687(5)	0.82(4)	−0.29(6)	−0.46(3)	1.98(8)
	OT/RNG [120]	0.697	0.947	−0.212	−0.462	2.106
	SP/MC [118]	0.23(1)	1.30(6)	0.72(4)		

at the ordinary transition and two different sets of critical exponents were obtained, see table 4. This dependence of the ordinary transition critical exponents on the surface orientation is explained by the fact that the bulk Lifshitz point is a strongly anisotropic equilibrium critical point.

One should note that various scaling relations are fulfilled for case A [115], such as for example

$$\gamma_s^L = \gamma_b^L + \nu_\parallel^L \tag{22}$$

$$\beta_s^L = \beta_b^L - \nu_\parallel^L \tag{23}$$

$$\gamma_s^L = 2\gamma_1^L - \gamma_{11}^L. \tag{24}$$

Here β_b^L, γ_b^L and $\nu_\parallel^L$ are Lifshitz point bulk critical exponents which take in the mean-field approximation the values $\beta_b^L = 1/2$, $\gamma_b^L = 1$ and $\nu_\parallel^L = 1/4$. Whereas (24) also holds for case B, the scaling relations (22) and (23) have to be modified in this case. Indeed, the behaviour of excess quantities is governed close to a bulk critical point by the bulk correlation length along the direction perpendicular to the surface. The Lifshitz point being an anisotropic critical point characterized by two correlation lengths diverging with different critical exponents, $\nu_\perp^L$ should be used in case B instead of $\nu_\parallel^L$. This then leads to the scaling relations

$$\beta_s^L = \beta_b^L - \nu_\perp^L \tag{25}$$

and

$$\gamma_s^L = \gamma_b^L + \nu_\perp^L. \tag{26}$$

Recent Monte Carlo simulations [118] revealed that the predictions of mean-field theory [115, 116] are qualitatively correct. As shown in table 4 the values of the surface critical exponents at the ordinary transition in the vicinity of the Lifshitz point indeed depend on the surface orientation. It is worth noting that for both surface orientations the value β_1^L for the surface order parameter is clearly smaller than the corresponding value obtained in the semi-infinite Ising model. Mean-field theory yields for all these cases the same value $\beta_1^{MF} = 1$.

Estimates for the Lifshitz point surface critical behaviour at the special transition point have also been included in table 4. Interestingly, the values of the critical exponents are very similar for the two different surface orientations. This is a strong indication that at the bulk Lifshitz point the surface critical behaviour at the special transition point may not depend on the orientation of the surface with respect to the axial axis. One may relate this observation to the fact that both the bulk (diverging bulk correlation length) and the surface (diverging correlation length for correlations along the surface layer) are critical at the special transition point. It may then be argued that the surface critical behaviour is governed to a large extent by the critical fluctuations along the surface, so that the surface orientation with respect to the direction of competing interactions is only of minor importance. At the ordinary transition, however, the surface is not critical and the surface critical behaviour is governed exclusively by the critical bulk fluctuations, leading to orientation-dependent critical exponents because of the anisotropic scaling at the bulk Lifshitz point.

Very recently Diehl and coworkers [119, 120] analysed the surface critical behaviour at bulk Lifshitz points using renormalization group methods. They thereby considered general m-axial Lifshitz points where the wave vector instability takes place in an m-dimensional subspace of the d-dimensional space. Thus for $m = 1$ one recovers the situation encountered in the ANNNI model. Restricting themselves to surfaces parallel to the modulation axes (i.e. to case B), they constructed the appropriate continuum $|\phi|^2$ models and computed the critical exponents at the ordinary transition to order ε^2. Their results for $m = 1$ are included in table 4. One notes very good agreement with the Monte Carlo results obtained in [118].

2.5. Critical dynamics at surfaces

Besides changing the local static critical behaviour surfaces also have an effect on the dynamic critical behaviour [122–138]. A central aspect of the works on dynamic surface critical behaviour concerns the possible classification of the distinct surface dynamic universality classes, similar to what has been done in the past for the dynamical bulk critical behaviour [139]. In that context semi-infinite extensions of the well-known bulk stochastic models are considered. Interestingly, different surface dynamic universality classes may be encountered for a given bulk model. This has especially been studied in the semi-infinite extension of the relaxation model B where the bulk order parameter is conserved [131, 132]. It has been shown that the presence of nonconservative surface terms, leading to a nonconserved local order parameter in the vicinity of the surface, yields a different dynamic critical universality class compared to the case where these terms are absent. These two universality classes share the same critical exponents but are characterized by different scaling functions of dynamic surface susceptibilities.

It is important to note that no genuine dynamic surface exponent exists [123]. Indeed all exponents describing the equilibrium critical behaviour of dynamic quantities can be expressed entirely in terms of static bulk and surface exponents and the dynamic bulk exponent z. For instance the dynamic spin–spin autocorrelation function decays for long times as $t^{-2x_1/z}$ where x_1 is the surface scaling dimension. The value of the dynamic exponent z is approximately 2.17 (2.04) in the two-dimensional (three-dimensional) Ising model.

The effect of surfaces on *non-equilibrium* dynamics after a quench from high temperatures, $T \gg T_c$, to the critical temperature has been investigated in [133, 134, 138]. These studies are to some extent complementary to the investigations of universal short-time behaviour in the bulk [140]. Indeed, similar to the bulk magnetization, the surface magnetization displays at early times a power-law behaviour

$$m_1(t) \sim m_{1,0} t^{\theta} \tag{27}$$

with $\theta = (x_i - x_1)/z$. Here $m_{1,0}$ is the small surface magnetization of the initial state, x_1 is the scaling dimension of the surface magnetization, whereas the non-equilibrium exponent x_i is the scaling dimension of the initial magnetization [140]. Corresponding power-law behaviour is also obtained for the local non-equilibrium autocorrelation in the long time limit $t \gg 1$ [133, 134]. It has been revealed recently [138] that in the case $x_i < x_1$ a new effect, called cluster dissolution, takes place, which leads to an unconventional, stretched exponential dependence of the short-time autocorrelation. A crossover to a power-law behaviour is then observed at later times. Interestingly, this stretched exponential behaviour is observed in the important case of the three-dimensional semi-infinite Ising model where $x_i = 0.53$ and $x_1 = 1.26$ [138].

There has been some progress in the analysis of dynamics in semi-infinite systems, but the situation is still very unsatisfactory as the effects of surfaces on dynamics have up to now only been studied in a very unsystematic way. From the experimental point of view the situation is even worse as no experimental studies of dynamic surface critical behaviour have yet been published. It has to be noted that some possible experiments, involving inelastic magnetic scattering of neutrons [141] or Mössbauer and NMR spectra [142], have been discussed in the literature, but they have not yet been realized.

2.6. Surfaces and fields

Up to this point we have only discussed surface phase diagrams in the absence of external fields. In fact, the global phase diagram not only depends on temperature and on the surface enhancement, but also on symmetry-breaking bulk and surface fields [10]. A discussion of the rich field of wetting phenomena, including for example critical wetting or prewetting, is beyond the scope of this review, even so some recent investigations of wetting criticality in wedge-shaped geometries will briefly be mentioned in section 3.3. The reader interested in this field is referred to the review by Dietrich [143] and to the overview of experiments by Bonn and Ross [144]. I also refrain from dealing with the related topic of localization–delocalization transitions observed for example in Ising films with competing surface fields. This topic was the subject of a recent review article by Binder *et al* [145].

Instead, I focus here on the normal transition and, especially, on the crossover between ordinary and normal transitions in the presence of weak surface fields. This crossover has attracted much interest in the past and is also of relevance when discussing recent experimental studies of surface critical behaviour.

At the normal transition the bulk orders at the bulk critical temperature in the presence of an ordered surface. The non-zero surface magnetization is thereby generated by a symmetry-breaking surface field. A similar situation is encountered at the extraordinary transition where the finite surface magnetization at the bulk critical temperature is due to strong enhancement of the surface couplings. These two different transitions have been shown [73, 74] to belong to the same surface universality class.

It seems natural to expect in the vicinity of the normal transition a monotonic decaying magnetization profile for $T \geqslant T_c$. This is indeed observed for strong surface fields, but for weak fields a more complex behaviour with a non-monotonic profile may be observed. Assuming that the surface enhancement c is subcritical, i.e. that without external fields one would be at the ordinary transition, it has been shown [146–148] that a small surface field leads to a short-distance increase of $m(z)$. This critical adsorption in systems with weak surface fields has been studied subsequently in a series of papers [149–153]. The increase of the layer magnetization is due to the fact that a weak surface field gives rise to a macroscopic length scale, yielding a power-law behaviour

$$m(z) \sim h_1 z^{\kappa} \qquad \text{with} \qquad \kappa = d - 1 - x_b - x_1 \tag{28}$$

where x_b and x_1 are the bulk and surface scaling dimensions, respectively. This increase continues up to a distance $l^{\text{ord}} \sim h^{1/(d-1-x_1)}$, where a crossover to the normal monotonic decrease $m(z) \sim z^{-x_b}$ sets in. Recent studies of critical adsorption in a weak surface field for a homologous series of critical liquid mixtures [154] have permitted observation of the predicted increase experimentally. It is worth noting that for surface enhancement corresponding to the special transition point $m(z)$ displays in the weak surface field limit a monotonic decay, but with two different power laws in the limits $z \longrightarrow 0$ and $z \longrightarrow \infty$ [155].

It has been suggested [148, 156] that this crossover between the ordinary and the normal transitions may explain some puzzling experiments on surface critical behaviour. In these experiments [53, 157] critical exponents compatible with the ordinary transition critical behaviour were measured, but at the same time the existence of residual long-range surface order was revealed at temperatures above the bulk critical temperature. This behaviour is readily explained by assuming that a weak surface field exists, yielding a surface structure factor governed by the ordinary behaviour in the case that l^{ord} exceeds the bulk correlation length. This interpretation assumes the existence of a surface field. It is therefore important to note that this kind of weak surface field can indeed arise in the studied compounds due to non-ideal stoichiometry effects [75, 158, 159].

3. Surfaces with edges and corners

The semi-infinite model with a flat surface may be considered to be a special case of a more complex wedge geometry where two planes meeting at an angle θ form an infinite edge. For $\theta = \pi$ the flat surface is recovered. Cardy showed that at the ordinary transition edge critical exponents depending continuously on θ arise on purely geometrical grounds [160]. For a given opening angle θ, however, the values of the critical exponents are expected to be universal and independent of microscopic details such as the strengths of the coupling constants or the lattice type. Whereas edge singularities at the ordinary transition have been studied intensively, especially in two dimensions [161], edge critical behaviour at the surface transition and at the normal transition have in general been overlooked. The recent investigations of edges and corners in systems with enhanced surface couplings and/or surface fields revealed some unexpected phenomena which will be reviewed in sections 3.2 and 3.3.

3.1. Ordinary transition

Cardy considered in his work d-dimensional $O(n)$ models containing edges formed by $(d-1)$-dimensional hyperplanes meeting at an angle θ [160]. For this geometry local critical exponents changing continuously with the angle θ are already obtained in the mean-field approximation. The edge magnetization critical exponent for example is given by

$$\beta_2^{MF} = \frac{1}{2} + \frac{\pi}{2\theta}. \tag{29}$$

For the opening angle $\theta = \pi$, the surface critical exponents are recovered. In the following, we use the same notation as Cardy and refer to edge quantities by the subscript 2. Corner quantities resulting, in dimensions $d \geqslant 3$, from the meeting of three hyperplanes will carry the subscript 3.

Near the bulk critical point T_c, the edge energy density has the scaling form [160]

$$f_e^{(\mathrm{sing})} = |t|^{(d-2)\nu_b}\psi(h|t|^{-\Delta_b}, h_1|t|^{-\Delta_1}, h_2|t|^{-\Delta_2}) \tag{30}$$

with $t = (T_c - T)/T_c$. ν_b is the critical exponent of the bulk correlation length, h, h_1, and h_2 are magnetic fields. h_2 only acts on edge spins, whereas h acts on all spins and h_1 on all surface spins. Δ_b and Δ_1 are the bulk and surface exponents appearing in the singular part of the free energy density of a semi-infinite system. The new exponent Δ_2, which has been computed in first order of an $\epsilon = d - 4$ expansion in [160], changes continuously with the wedge angle θ. All edge critical exponents may be expressed by Δ_2 together with bulk and surface critical exponents. From the renormalization group point of view, the angle dependence has its origin in the invariance of the edge under rescaling. This makes the opening angle a marginal variable and may therefore lead to angle dependent local critical exponents.

Inspired by these results, subsequent work mainly studied the influence of 'edges' in two dimensions. In the following only some selected results obtained in two dimensions are discussed, the interested reader is referred to the excellent review of Iglói, Peschel and Turban [161] for a more complete account. The 'edge' then reduces to one point and forms a corner in a two-dimensional system. Based on numerical and analytical calculations of isotropic two-dimensional Ising models [162], the critical exponent of the local edge magnetization was postulated to be

$$\beta_2 = \frac{\pi}{2\theta} \tag{31}$$

for two-dimensional Ising models. A similar equation was proposed for anisotropic lattices, with the opening angle replaced by an effective angle depending on the ratio of the different couplings. Using the conformal transformation $w = z^{\theta/\pi}$, which transforms the semi-infinite system in the z-plane to a wedge with opening angle θ in the w-plane, a simple relation between edge and surface critical exponents in two dimensions was derived [57, 162]. Thus, for the local magnetization one obtains

$$\beta_2 = \frac{\pi}{\theta}\beta_1 \tag{32}$$

which is in accordance with equation (31) for the Ising model. Other work focused on the temperature behaviour of the local magnetization in two-dimensional Ising models with various opening angles and lattice types [163–166]. Up to now a complete solution has only been obtained for the square lattice Ising model with $\theta = \pi/2$ [167–169]. Further studies also investigated the influence of edges in other two-dimensional systems. Examples are polymers [170, 171], regarded as $O(n)$ models in the limit $n \longrightarrow 0$, or Potts models [172].

Qualitatively different critical behaviour is observed in systems with parabolic shapes [161, 173]. These systems have the remarkable property that they are asymptotically narrower than wedges. In this geometry one does not observe the usual power laws at criticality but stretched exponentials. Close to the critical point the tip magnetization vanishes like $\exp(-at^{-b})$ with $a, b > 0$ and $t = (T_c - T)/T_c$.

For small three-dimensional systems, edges and corners may be expected to play a dominant role, for instance, in nanostructured materials. Studies to reproduce average properties of such small clusters of atoms have been performed. These include several Monte Carlo investigations (see, e.g., [174–176]). Critical phenomena at edges in three-dimensional models have, however, been addressed only rarely. Most investigations of edge criticality focused on Ising models, but some studies of percolation [177, 178] and of polymers [170, 179] in three-dimensional wedges have also been published. Whereas most of these studies of edge critical properties investigated the case that at the bulk critical point both surfaces forming the edge undergo an ordinary transition, Wang *et al* [180] also computed critical exponents for the cases that at least one of the surfaces undergoes a special transition. In this renormalization group study, the authors limited themselves to the opening angle $\theta = \pi/2$. They also studied the corner critical behaviour of cubic systems, each surface having von Neumann (special transition) or Dirichlet (ordinary transition) boundary conditions. Saxena [181] discussed, based on renormalization group calculations, the possible phase diagrams of Ising models with an edge formed by two perpendicular surfaces. Similar methods were used by Larsson [182] in his study of Ising edge critical behaviour, limiting himself mainly to the ordinary transition. The edge exponent $\Delta_2(\theta)$, see equation (30), was computed for some angles θ by Guttmann and Torrie [170] using high temperature series

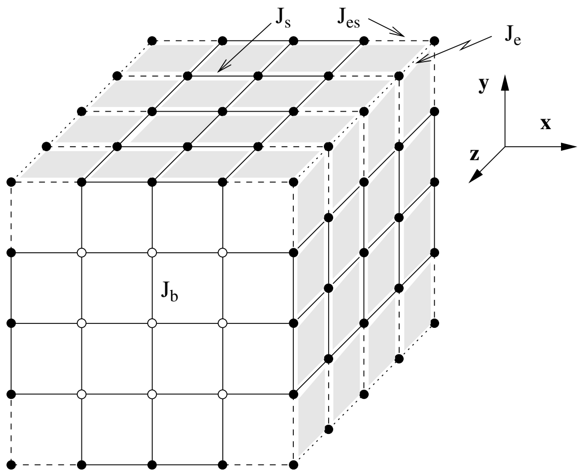

Figure 4. Geometry of a model with (100) and (010) surfaces, i.e. edges with opening angles $\theta = \pi/2$. J_b and J_s are the bulk and surface couplings, respectively. J_e is the coupling between neighbouring edge spins, J_{es} the coupling between an edge spin and its neighbouring surface spin.

expansions. Based on these results, they proposed an expression for $\Delta_2(\theta)$ supposed to be valid for all θ. Early Monte Carlo simulations of Ising models were done by Mon and co-workers in order to compute the edge exponent $\Delta_2(\theta = \pi/2)$ [183] as well as the corresponding corner quantity Δ_3 for a cube [184]. In these studies, only rather small systems were investigated. The critical free energies of Ising models with edges and corners were also studied [185, 186], following a similar investigation in two-dimensional critical systems with corners [187]. $O(n)$ models with edges and corners were studied in the limit $n \longrightarrow \infty$ in [188]. The temperature dependence of the edge and corner magnetizations as well as related quantities were only investigated recently for three-dimensional Ising models in the case of equal surface and bulk couplings [189, 190], using modern simulation methods.

To introduce edges in Ising magnets, periodic boundary conditions along one axis, the z-axis, are applied. The remaining four free surfaces of the crystal may be oriented in various ways leading to different opening angles θ at the edges. As shown in figure 4, pairs of (100) and (010) surfaces lead to four equivalent edges with opening angles $\theta = \pi/2$. The intersections of (100) and (110) surfaces form two pairs of edges with $\theta = \pi/4$ and $\theta = 3\pi/4$. This is illustrated in figure 5. Besides the bulk coupling J_b and the surface coupling J_s, further couplings may be introduced [189, 191]: two neighbouring edge spins interact with the edge coupling J_e, whereas an edge spin is coupled to its neighbouring surface spin by the edge–surface interaction J_{es}. When studying edge behaviour near the ordinary transition all couplings can be considered to have the same strength: $J_e = J_{es} = J_s = J_b$.

The values of the local critical exponent β_2 of the edge magnetization obtained in various studies of Ising models are compiled in table 5. The expected angle dependence of the local critical exponents is thereby nicely illustrated. The values given by mean-field theory are systematically too high, according to the predictions of the renormalization group [160]. These predictions, in turn, seem to be systematically too large, as suggested both by high-temperature series expansions [170] and by Monte Carlo simulations [189]. The last two methods yield results which are in close agreement with each other. The value of β_2 for $\theta = \pi/2$ derived from the Monte Carlo study of Mon and Vallés [183] differs significantly

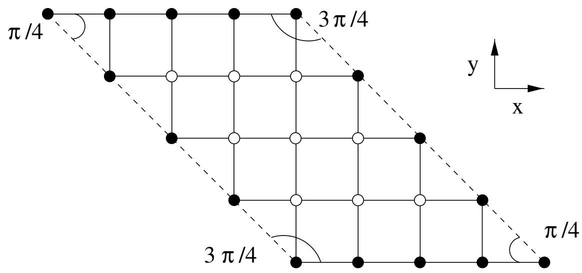

Figure 5. Geometry of a model with edges with opening angles $\theta = \pi/4$ and $\theta = 3\pi/4$. Shown is a cut through the crystal perpendicular to the edge direction. The full lines show the couplings between neighbouring spins, whereas the (110) surfaces are indicated by the dashed lines.

Table 5. Predictions for the Ising edge magnetization critical exponents from various methods for four different opening angles of the three-dimensional wedge. MF: mean-field approximation, RNG: renormalization group theory, HTS: high-temperature series expansions, MC: Monte Carlo simulations.

	$\pi/4$	$\pi/2$	$3\pi/4$	π
MF [160]	2.50	1.50	1.17	1.00
RNG [160]	2.48	1.39	1.02	0.84
HTS [170]	2.30	1.31	0.98	0.81
MC [183]		1.38(6)		
MC [189]	2.3(1)	1.28(4)	0.96(2)	0.80(1)

from the value obtained from the recent studies using cluster algorithm [189], presumably due to the small systems investigated in that early study.

In order to study the universality of the computed critical exponents, one may investigate, at a fixed opening angle, wedges which are formed by different pairs of surfaces. For example, comparing $\theta = \pi/2$ edges formed by (100) and (010) surfaces or (110) and $(1\bar{1}0)$ surfaces shows that, on the one hand, the local magnetizations differ, but that, on the other hand, the values of the local critical exponents are invariant against rotation of the crystal [189]. Note that the invariance of boundary critical exponents against rotation of the crystal has been discussed and partly even proved for edges in two-dimensional Ising models [161, 163]. Similarly, modifying the strength of the couplings does not alter the values of the critical exponents at the ordinary transition [189]. Furthermore, changing the lattice type is not supposed to change the critical behaviour either. The independence of the values of the edge critical exponents from the lattice type has been studied in two dimensions [161].

Investigations of critical phenomena near corners in three-dimensional systems have up to now been limited to the special case where the three surfaces forming the corner are mutually perpendicular. In Monte Carlo simulations, Ising cubes on simple cubic lattices with free surfaces are considered [184, 189, 192]. The corner magnetization critical exponent is thereby determined to be $\beta_3 = 1.77(5)$ [192]. This value is significantly lower than the mean-field value $\beta_3^{MF} = 2$ [161]. Analytical results beyond mean-field are not yet available.

Recent simulations of water in hydrophobic pores also illustrated the effect of curved surfaces on the values of local critical exponents [193]. In that study Brovchenko *et al* observed a sharp crossover for cylindrical surfaces, yielding an asymptotic value for the local order parameter larger than the value $\beta_1 \approx 0.82$ measured for slit-like pores. The critical behaviour characteristic of the ordinary transition is expected to be observed in this case not too close to T_c as one is dealing with the liquid–vapour transition near a weakly attractive surface, see the discussion in section 2.6. Of course, the geometry is slightly different to the wedge-shaped geometries discussed so far in the literature, but nevertheless the kind of system discussed in [193] seems to be a good candidate to study the effect of (generalized) edges on the local critical behaviour experimentally in the future.

3.2. Surface transition

Edge and corner critical properties at the surface transition have been usually overlooked. This problem was briefly addressed in [182] and [181], but no systematic study has been done until recently [191, 192]. As shown in the following, intriguing phenomena are observed at edges and corners when the surface orders whereas the bulk remains disordered. Especially, non-universal local critical exponents are encountered at the surface transition of crystals with edges and corners. As discussed in section 3.1, edge and corner critical exponents at the ordinary transition depend on the opening angle but do not depend on microscopic details of the model, such as for example the values of the interactions, the lattice type or the orientation of the surfaces. The edge and corner behaviour at the surface transition is in marked contrast to this, as, for a fixed opening angle, local critical exponents change continuously with the strengths of the different couplings [191, 192]. As we shall see, the values of edge and corner critical exponents at the surface transition also reflect the existence of the disordered bulk.

At the surface transition of the three-dimensional semi-infinite Ising model with a perfect surface, the critical fluctuations are essentially two dimensional. The surface critical exponents reflect this reduced dimensionality, e.g. $\beta_1 = \beta_{2D} = 1/8$. On the other hand, the edge presents a local perturbation, acting presumably like a line defect in a two-dimensional system. Simple one-dimensional defects in the two-dimensional Ising model have been studied intensively [194–202]. It was shown that in the vicinity of these defects the local magnetic critical exponents are non-universal [195]. As these exact results provide a useful framework for discussing the numerical findings of [191] and [192], I briefly review in the following the main results concerning the local critical behaviour near defect lines in two-dimensional Ising models.

The plane Ising model with a defect line [194] is an interesting system displaying non-universal magnetic critical exponents. A simple analysis on the relevance of perturbations shows that in two-dimensional Ising models an energy-like one-dimensional perturbation is marginal, yielding continuously varying local critical exponents. This is a consequence of the fact that in the unperturbed system the correlation length critical exponent ν_b equals 1 and the scaling dimension of the surface magnetization operator x_1 is equal to 1/2 [161]. The non-universal behaviour was proved for the first time by Bariev [195]. He analysed two types of defect lines: chain defects, where a column of perturbed couplings with strength J_{ch} is considered, and ladder defects, where modified couplings of strength J_l connect spins belonging to two neighbouring columns. Bariev's exact results demonstrate the dependence of the local magnetization critical exponent on the values of the defect coupling. For the ladder defect, the local critical exponent is

$$\beta_l = \frac{2}{\pi^2} \arctan^2\left(\kappa_l^{-1}\right) \tag{33}$$

with

$$\kappa_l = \tanh\left(\frac{J_l}{k_B T_{2D}}\right) \Big/ \tanh\left(\frac{J}{k_B T_{2D}}\right) \tag{34}$$

whereas for the chain defect one obtains

$$\beta_{ch} = \frac{2}{\pi^2} \arctan^2(\kappa_{ch}) \tag{35}$$

Table 6. Ising edge critical exponents β_2 at the surface transition for systems with opening angles $\theta = \pi/2$ and $J_s = 2J_b$. J_l^{eff} is the effective defect coupling of a ladder defect having the same critical exponent as the edge.

	$J_{es} = J_s, J_e = J_s$	$J_{es} = J_s/2, J_e = J_s$	$J_e = J_s/2, J_{es} = J_s$
β_2	0.095(5)	0.176(5)	0.127(5)
J_l^{eff}	$1.22J_s$	$0.74J_s$	$0.99J_s$

with

$$\kappa_{ch} = \exp\left(-2\left(\frac{J_{ch}}{k_B T_{2\text{D}}} - \frac{J}{k_B T_{2\text{D}}}\right)\right). \tag{36}$$

J is the strength of the unperturbed interactions, whereas $T_{2\text{D}}$ is the critical temperature of the two-dimensional Ising model. For both cases, enhanced (reduced) defect couplings yield a lower (higher) local critical exponent as compared to the perfect two-dimensional Ising model, $\beta_{2\text{D}} = 1/8$.

In the following, I discuss the influence of edges with opening angle $\theta = \pi/2$, see figure 4, on the local critical behaviour at the surface transition. Because edges are one dimensional, and all couplings in the models are short range, edge quantities only become singular at the temperature T_s where the surface orders. Near the surface transition, where the critical fluctuations are of two-dimensional character, the edge then acts like a defect line in an essentially two-dimensional bulk Ising model. The edge coupling J_e corresponds to a chain-like defect, the edge–surface coupling J_{es} to a ladder-type defect. The change in the topology at the edge compared to the surface amounts to a complicated ladder-type defect.

The value of the critical exponent is non-universal, it varies continuously as a function of the coupling strength J_{es} as shown in table 6. These findings may be related to the reported results for two-dimensional Ising models with a ladder defect. The ladder corresponds to the edge, and the ladder coupling J_l reflects not only the edge–surface interaction J_{es} but also the reduced connectedness to bulk spins at the edge compared to the surfaces. For $J_{es} = J_e = J_s$ and $J_s = 2J_b$, the critical exponent of the edge magnetization has the value $\beta_2 = 0.095(5)$, significantly lower than the critical exponent of the perfect two-dimensional Ising model. Comparing the local critical exponent β_l near a ladder defect, see equations (33) and (34), with β_2, one may attribute an effective ladder coupling J_l^{eff} to the edge with $J_l^{\text{eff}} > J\ (=J_s)$. This effective enhancement of the couplings is due to the influence of the bulk spins. When lowering the coupling J_{es} while keeping J_s and J_b constant, the value of β increases, as expected from equation (33), see table 6. The weakening of the edge interaction J_e has a less pronounced impact on β_2 than the weakening of J_{es}. The close agreement of β_2 with $\beta_{2\text{D}}$ in the case $J_e = J_{es}/2$ is fortuitous. It is due to a compensation of a reduction in β_2 following from the increase in the effective ladder coupling stemming from the edge topology, and of an enhancement in β_2 following from the decrease in the strength of the edge coupling.

At the surface transition of three-dimensional Ising models corner criticality deserves to be analysed as well. As edges are local perturbations acting similar to defect lines in two-dimensional models, the corners of a cube may be interpreted as intersection points of three defect lines. As shown in table 7 one again obtains critical exponents changing continuously with the strengths of the different couplings.

To explain these findings, note that the corners are intersection points of edges and recall that at the surface transition the critical fluctuations are essentially two dimensional. The

Table 7. Ising corner critical exponents β_3 at the surface transition for systems with opening angles $\theta = \pi/2$ and $J_s = 2J_b$. $\beta_{\rm star}$ is the local critical exponent near a star defect where three ladder defects with defect couplings $J_l^{\rm eff}$, see table 6, intersect.

	$J_{es} = J_s, J_e = J_s$	$J_{es} = J_s/2, J_e = J_s$	$J_e = J_s/2, J_{es} = J_s$
β_3	0.06(1)	0.26(2)	0.14(2)
$\beta_{\rm star}$	0.082	0.210	0.128

critical exponent of the corner magnetization, β_3, has been related to that of the magnetization at the intersection of three semi-infinite defect lines in the two-dimensional Ising model. The critical exponent $\beta_{\rm star}$ for star defects formed by three intersecting ladder defects has been calculated by Henkel *et al* [203, 204]. One may assign to the edges an effective ladder coupling $J_l^{\rm eff}$ by setting $\beta_l = \beta_2$. Inserting this effective coupling into the equation derived for a star defect formed by three ladder defects [203, 204] then gives $\beta_{\rm star}$. The comparison of β_3 with $\beta_{\rm star}$ yields a satisfactory agreement, see table 7. Of course, a more refined analysis would focus on the fact that the correct geometry of the present problem is not that of a plane but that of a cone with three defect lines meeting at an angle $\pi/2$ [205] (see [206] for a recent discussion of Ising models with conical singularities). Furthermore, the rather complicated nature of the edge as a simultaneously ladder- and chain-type defect line as well as the effect of the bulk spins on the corner magnetization should then also be taken into account.

3.3. Wedges and surface fields

The critical behaviour near edges has also been studied recently at the normal transition [213]. The authors investigated critical adsorption near edges due to the presence of symmetry-breaking surface fields in a wedge. Besides studying the problem in the mean-field approximation, they also presented some exact results for the two-dimensional case. Especially, the critical edge exponent β_2 was discussed. It was shown that at the normal transition local critical exponents also depend continuously on the opening angle.

Critical adsorption near edges is, however, only one of the many intriguing phenomena encountered in systems with both wedges and surface fields. In the case of adsorption of a fluid on a solid substrate with wedge geometry [214, 215] it is expected from thermodynamic arguments that the liquid fills the wedge completely at temperatures $T > T_F$, where the filling temperature T_F is lower than the wetting temperature T_W of a planar, but otherwise identical, wall [216]. In a series of recent papers Parry *et al* [217–221] studied the corner filling transition in detail, focusing especially on fluctuation effects and on the universality classes of filling transitions. One of their predictions was that critical filling, i.e. the filling transition for $T \longrightarrow T_F^-$, could be continuous even in cases where the related wetting transition is of first order. They also studied the divergence of various length scales associated with this phase transition and predicted, based on a fluctuation theory, that the interfacial height l_0 from the bottom of the wedge should diverge as $l_0 \sim (T_F - T)^{-1/4}$ [218, 222].

The wedge filling transition can be studied in Ising models with wedge geometries by applying surface fields which favour one of the two phases in the wedge [223–226]. Exact results in the two-dimensional case [224] permit the establishment of the existence of this kind of transition. Recent numerical investigations [225, 226] revealed very good agreement with the theoretical predictions of Parry *et al*. In addition, a new type of interface localization–delocalization transition was revealed in the three-dimensional double wedge forming a pore with a square cross section [226]. The critical exponents of this transition can be related to the critical exponents of the filling transition in a simple wedge.

3.4. Non-equilibrium systems

The influence of wedges on critical behaviour has not only been studied in equilibrium systems but also in non-equilibrium systems. Fröjdh *et al* [207] introduced an edge into a directed percolation process and analysed the impact this edge has on the non-equilibrium phase transition observed in this system. This work generalized earlier studies of directed percolation in a semi-infinite geometry [208] to the wedge geometry. Angle-dependent edge critical exponents were observed in this non-equilibrium case, too. Directed percolation processes have also been studied in two-dimensional parabolic-like systems with a free surface at $y = \pm Cx^k$ [209, 210]. For $k < 1/z$, z being the dynamical exponent, the surface shape is a relevant perturbation and the tip order parameter displays stretched exponential behaviour. In the marginal case, $k = 1/z$, non-universal local critical behaviour is again observed.

Other non-equilibrium absorbing phase transitions have also been studied in semi-infinite systems recently [211, 212], but these studies have not been extended to wedge-shaped geometries.

4. Critical phenomena at non-perfect surfaces

In the preceding sections we discussed critical phenomena in systems with various geometries: semi-infinite systems, wedge-shaped systems and cubes. All the results presented so far have in common that only idealized, perfect surfaces were considered. However, real surfaces are often naturally rough, as steps or islands occur during growth processes or result from the effect of erosion. Furthermore, methods from nanoscience permit the creation of artificial structures on top of films. Examples include lines of adatoms or regular arrangements of geometric structures. All these defects have some impact on magnetic surface quantities.

In the following, I review theoretical studies where surface critical phenomena in systems with various surface defects have been investigated. Section 4.1 deals with semi-infinite (i.e. bulk terminated) systems, whereas section 4.2 is devoted to the influence of surface defects on the critical behaviour of (ultra)thin films.

4.1. Semi-infinite systems with surface imperfections

Geometric surface imperfections (e.g., islands or vacancies) and impurities may be stable on the time scale of magnetic phenomena and thus lead to quenched surface disorder [227]. Some experiments indicate an enhancement of disorder near surfaces, thus pointing to the possible realization of quenched surface disorder in systems where bulk disorder is negligible. In a theoretical description, this kind of surface disorder is usually mimicked by random surface fields or by random surface couplings.

Early studies mainly focused on the global phase diagram observed in systems with random surface couplings or random surface fields. In [228] dilute semi-infinite Ising models with bond and site dilution both in the bulk and at the surface were considered. Mean-field results obtained for semi-infinite Ising models with random surface and bulk fields were presented in [229]. The possible types of phase diagrams were established and the phase transitions as well as multicritical points were discussed. Phase diagrams obtained for semi-infinite transverse Ising models with random surface and bulk fields were analysed recently in [230].

In a series of papers, Kaneyoshi (see, e.g., [231–233]) studied semi-infinite Ising systems with an amorphous surface layer in detail. The amorphous surface can be mimicked by choosing randomly weak or strong nearest-neighbour ferromagnetic couplings between surface spins. Sometimes, he also considered random couplings between surface spins and the underlying bulk spins. Using different analytical approaches, surface magnetic properties, such as, for example, the magnetization of the surface layer, were analysed. The corresponding phase diagrams were derived from the results of an effective field theory which includes correlations. One interesting result obtained in these studies concerns the location of the special transition point. Kaneyoshi observed that the critical coupling ratio r_{sp} is shifted to higher values in systems with a diluted surface and he conjectured that this is a common effect of surface amorphization. This was confirmed by a Monte Carlo study [8] where the strength of surface bonds was chosen randomly between two different values J_{s1} and J_{s2}, the ratio $d = J_{s1}/J_{s2}$ measuring the degree of dilution. For $d = 1/10$ the special transition point is located at the mean coupling ratio $r_{sp} = 1.7(1)$ for the simple cubic lattice, noticeably larger than the value obtained for the perfect surface $r_{sp} \approx 1.5$, see section 2.1. In order to understand this shift we recall that in the limit $r = (J_{s1} + J_{s2})/(2J_b) \gg 1$ the surface effectively decouples from the underlying bulk and can be regarded as a two-dimensional system. However, it is well known that at a given mean coupling $(J_{s1} + J_{s2})/2$ the critical temperature of the two-dimensional Ising model is reduced by randomness [234]. Therefore, for fixed r, increasing randomness shifts the line of the surface transition to lower temperatures which in turn shifts the location of the special transition point to larger values of the coupling ratio.

Sometimes, alloy surfaces are mimicked by semi-infinite surfaces with randomly decorated magnetic and nonmagnetic atoms located at the surface [235]. Again, the location of the special transition point is observed to shift as a function of the model parameters. Quantities having an impact on this shift are for example the concentration of the nonmagnetic surface atoms or the spin of the magnetic atoms.

The investigations reviewed so far almost exclusively focused on global phase diagrams of semi-infinite systems with non-perfect surfaces. The different authors did not try to study in detail the influence of these imperfections on the surface critical behaviour. However, as a certain degree of imperfections is unavoidable when studying surfaces experimentally, it is very important to clarify whether the surface critical exponents are robust against surface imperfections.

A first step in this direction was taken by Mon and Nightingale in their study of the influence of a random surface field on the surface critical behaviour of the semi-infinite Ising model [236]. This work was motivated by the determination of the surface order parameter critical exponent β_1 in a study of wetting phenomena of binary mixtures consisting of a polar and a nonpolar liquid [237]. The value obtained for β_1 in that study was compatible with the value encountered in the semi-infinite Ising model with a perfect surface, even so β_1 described the vanishing of the surface order parameter in the presence of a random surface field with zero average strength. Using a Harris-type criterion [238], Mon and Nightingale conjectured that, at the ordinary transition, a random surface field is irrelevant for the surface critical behaviour of the Ising model. They verified their prediction with the aid of Monte Carlo simulations. Using renormalization group techniques it was shown in [239] that surface bond-dilution is irrelevant for the semi-infinite Ising model, the universality classes of the different transitions being those of the pure system.

In an extensive study, Diehl and Nüsser [227] derived Harris-type criteria for various types of quenched surface disorder with the aim of assessing the relevance or irrelevance of these random imperfections on the pure system surface critical behaviour. In his original work, Harris [238] studied the stability of critical bulk systems in the presence of randomness. The well-known Harris criterion states that, in the weak-disorder limit, bond disorder is irrelevant for the bulk critical behaviour provided the specific heat critical exponent α is negative. Disorder is relevant for $\alpha > 0$, whereas the case $\alpha = 0$ is marginal. Looking at the Ising model, one concludes, based on the Harris criterion, that in three dimensions disorder is relevant as $\alpha \approx 0.11$, whereas in two dimensions one encounters the marginal case $\alpha = 0$ which has attracted much interest [240]. One should note that the condition for irrelevance of disorder resulting from a Harris-type criterion is a necessary but not a sufficient condition for the stability of the pure system's critical behaviour. Nevertheless, a Harris-type criterion is usually a reliable indicator for the irrelevance of randomness.

The Harris criterion generalized in [227] to the surface critical behaviour states that short-range correlated disorder is relevant or irrelevant depending on whether some (surface) susceptibility, which depends on the kind of randomness under investigation, diverges or is finite at the critical point. For random surface fields the quantity of interest is the surface susceptibility χ_{11} of the pure system, whereas for random surface couplings the relevant susceptibility is the local specific heat C_{11} [3]. As these generalized susceptibilities have a singularity of the form

$$X_{11} \sim |T - T_{\rm c}|^{-\Gamma_{11}} \tag{37}$$

at the critical point, the criterion indicates that the disorder is relevant for positive Γ_{11} (i.e. γ_{11} or α_{11}), but that it is irrelevant for negative Γ_{11}.

This criterion has been applied by Diehl and Nüsser in various cases involving surfaces. Thus, the presence of random surface fields is expected to be irrelevant at the ordinary transition for all $O(n)$ models with $n \leqslant 3$ if the dimension $d > 2$, in accordance with the results obtained by Mon and Nightingale [236] for the special case of the semi-infinite Ising model ($n = 1$). Interestingly, Feldman and Vinokur recently showed [241] that weak quenched surface disorder destroys bulk ordering in the case of a system with continuous symmetry (such as the XY model), leading to a power-law decay of correlation functions and therefore to the appearance of quasi-long-range order. In the two-dimensional semi-infinite Ising model, the perturbation caused by the random surface field is marginal so that the criterion does not yield a definite answer. This case was studied subsequently in [242–245] where it was shown that the surface critical behaviour of the two-dimensional Ising model is described by Ising critical exponents with logarithmic corrections to scaling. For the special transition point, the Harris-like criterion of [227] indicates that random surface fields are relevant in dimensions $d \leqslant 4$. However, the three-dimensional semi-infinite Ising model with quenched random surface fields does not present a special transition point nor an extraordinary transition, as the surface transition line, where the surface orders alone, does not exist anymore. This follows from the fact that at finite temperatures random bulk fields destroy long-range order in the two-dimensional bulk Ising system [246]. In the cases where the extraordinary transition still exists in the presence of random surface fields, the criterion predicts that the disorder is then irrelevant. For random surface couplings, the perturbation is found to be irrelevant both at the ordinary and at the extraordinary transitions. More interesting is the situation at the special transition point where early estimates of the critical exponent α_{11} in three dimensions yielded small negative [16, 247] *or* small positive values [3], implying that short-range enhancement disorder is close to being relevant in three dimensions. Recently, new field-theoretical estimates also resulted in negative values for α_{11} [43, 44]. The Monte Carlo results obtained for three-dimensional semi-infinite Ising models with random surface-bond disorder [8] are also compatible with the irrelevance of random surface enhancement for the special transition point critical behaviour. However, as short-range random surface enhancement is close to being relevant, one might expect long-range correlated enhancement disorder to be relevant at the special transition point [227].

Diehl and Nüsser also studied the impact of surface-enhancement disorder at the special transition of a bulk tricritical system. As in this case the Harris criterion did not permit a

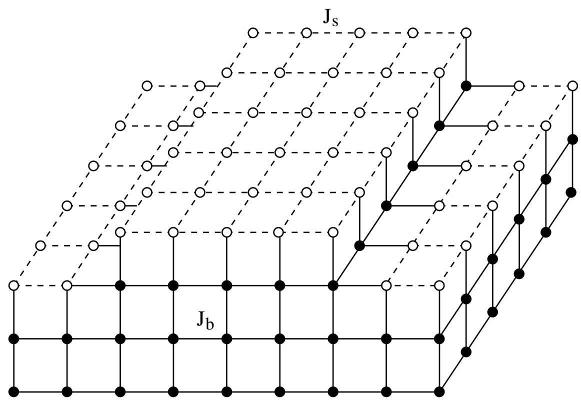

Figure 6. Geometry of a model with two straight steps of monatomic height. J_b and J_s are the ferromagnetic bulk and surface couplings, respectively.

definite prediction, renormalization group techniques were used in a second paper [248] to clarify the situation.

The robustness of the surface critical exponents at the ordinary transition against two types of surface imperfections was established in a Monte Carlo study [8]. The studied imperfections correspond to an amorphous surface, mimicked by random strong and weak couplings in the surface, and to a simple case of corrugation, due to the presence of a step of monoatomic height superimposed on a perfect surface. For the amorphous surface, the Monte Carlo results showed that the dilution, at a fixed temperature $T < T_c$, decreases the magnetization at and near the surface. The effective critical exponent, derived from the magnetization of the diluted surface, closely follows in the Ising case that of the perfect case, yielding the same asymptotic value $\beta_1 = 0.80(1)$. Randomness in the surface couplings is therefore irrelevant for the asymptotic behaviour of the surface magnetization, and even of minor importance for the corrections to scaling [8]. Similarly, the estimate for surface susceptibility critical exponent γ_1 is compatible with the one in the perfect case. These numerical findings provide support for the conjecture of [227] that the surface enhancement disorder is irrelevant at the ordinary transition. The robustness of the critical exponent β_1 against dilution observed in the numerical study was later proved by Diehl [249] who derived upper and lower bounds on the magnetization of the diluted surface and showed in a rigorous way that β_1 takes the same value in the diluted system as in the perfect system.

In [8] the effect of corrugation on the surface critical behaviour was studied in Ising systems where an extra half layer in the form of a strip-like terrace of monoatomic height was superimposed on a perfect surface, as shown in figure 6. For this geometry the magnetization at the step-edge deviates most significantly from the magnetization of the perfect surface. The local critical exponent describing the behaviour of the step-edge magnetization was found to have the value 0.800(15), in agreement with that of the magnetization of the flat surface. However, in contrast to the case of random couplings, corrections to scaling are here distinctively different from those of the perfect surface. Diehl also considered this type of imperfection in [249] and showed in a rigorous way that the critical exponent of the step-edge magnetization is identical to that of the magnetization of a perfect surface. Note that at the surface transition local critical magnetic exponents are expected to be non-universal close to the step-edge. Indeed, the step-edge should then act like a defect line in a system governed by two-dimensional critical fluctuations. This is supported by Monte Carlo simulations which yield for $J_s = 2J_b$ the value 0.33(2) for the step-edge magnetization critical exponent [90] in the Ising model.

The study of magnetic properties of rough, corrugated surfaces near criticality is a rather new and promising field. The case of one additional terrace on an otherwise perfect surface may be generalized to the more complex situation of vicinal surfaces with terraces separated by equally spaced monoatomic steps [250–253]. In nature, rough surfaces often result from a growth process and strongly affect the surface magnetization. Diffusion-limited growth results in a rough growth front following a Poisson distribution. This may be realized in simulations by considering a surface formed of columns of random heights [251], see also [254]. Layer-by-layer growth, however, may result in films with a finite number of complete layers and one partially filled layer, thus yielding a different type of roughness [255]. Whereas the different kinds of roughnesses discussed so far have been shown to be (or are supposed to be) irrelevant for the surface critical behaviour at the ordinary transition, this is not always the case. In a recent interesting work, Hanke and Kardar [256, 257] showed that self-affine rough surfaces may give rise to novel surface critical behaviour with surface critical exponents different from those of the perfect case. Similar results have previously been obtained in two-dimensional systems with fractal boundaries [258, 259] yielding new multifractal boundary exponents. These results in two dimensions have been interpreted in terms of a scale-dependent distribution of opening angles of the fractal boundary [259]. The same analogy has been evoked in the discussion of the surface critical behaviour of self-affine surfaces in [256, 257].

Hanke and Kardar also studied critical correlations in the vicinity of a regularly patterned surface (as might for example result from a lithographic preparation of the surface). Using a perturbative calculation in the deformations in height from a flat surface they showed that the leading power-law decay of the correlations is the same as for a flat surface, but with a modulated amplitude reflecting the shape of the surface [256, 257].

Extended surface defects have been studied intensively in two dimensions. In the Hilhorst–van Leeuwen model [260, 161] one considers a semi-infinite square lattice with inhomogenous couplings (alternatively, the triangular lattice has also been investigated). In the direction parallel to the surface one has couplings with a constant strength J_1, whereas the strength of the couplings varies perpendicular to the surface as a function of the distance y to the surface:

$$J_2(y) - J_2(\infty) = \frac{A}{y^\omega}. \tag{38}$$

This extended perturbation is irrelevant for $\omega > 1/\nu_b = 1$, yielding the same critical behaviour as the homogeneous semi-infinite system. For $\omega < 1$, however, the perturbation is relevant and a spontaneous surface magnetization is observed at the bulk critical point. The most interesting case is $\omega = 1$, where the perturbation is marginal. Here spontaneous surface magnetization is again observed for values of A larger than some threshold A_c, whereas for $A < A_c$ the scaling dimension x_1 varies continuously as a function of A: $x_1 = \frac{1}{2}(1 - A/A_c)$. This intriguing behaviour has attracted much interest in the past [161] and has recently led to the discovery of an up to then unnoticed effect in the short-time non-equilibrium critical dynamics at surfaces [138].

Finally, before turning to thin films with surface imperfections, let us briefly mention some recent work concerning the surface critical behaviour in an Ising model with quenched random defects in the bulk. In the three-dimensional bulk Ising model, the quenched random defects are a relevant perturbation leading to modified critical bulk exponents [261, 262]. The surface critical behaviour of the three-dimensional Ising model with quenched bulk disorder has been investigated both at the ordinary [263, 264] and at the special transition point [263, 265], using different renormalization group techniques. The crossover behaviour between these two transitions was studied recently in [266]. Interestingly, modified surface critical behaviour is encountered independently of whether quenched surface disorder is present or not. The corresponding marginal case $d = 2$ has also been studied in detail recently [267, 268], yielding Ising surface critical exponents with logarithmic corrections to scaling. Boundary critical behaviour of q-state random Potts models has been studied in [269] for $3 \leqslant q \leqslant 8$. It should be noted that the problem of bond percolation has also been investigated in semi-infinite geometries [32–36]. In this case distinct surface percolation transitions have been identified and the values of the local critical exponents have been computed.

4.2. Thin films with surface imperfections

In a series of papers Aarão Reis studied the dependence of physical quantities in two-dimensional Ising stripes [270–273] and three-dimensional Ising thin films [254, 255] on the surface roughness. Using transfer matrix methods, Reis investigated stripes where the column heights were chosen according to a Gaussian distribution with mean L (L: integer) and variance $(\Delta L)^2/2$ [270, 271]. Two different cases were considered: ΔL constant and $\Delta L = L/L_0$ with some constant L_0. Whereas the roughness becomes unimportant for large L in the former case, in the latter case the roughness increases with the mean thickness. Reis paid special attention to the finite-size scaling and to the finite-size corrections due to randomness. In [272], he also considered the case of noninteger mean L and showed that the free energy displays interesting oscillating behaviour as a function of continuously changing L due to oscillations in the mean coordination number. Recently [273], he completed his investigation of stripes of random width by studying roughness of the more general form $\Delta L \sim L^\beta$ with $0 \leqslant \beta \leqslant 1$. He also considered correlated roughness by imposing the maximal height difference between neighbouring columns to be not larger than one-lattice constant. Interestingly, these computations showed that the correlations had no systematic effect on the corrections to scaling. More relevant to the understanding of the critical behaviour of real films are Reis' studies of films with rough surfaces [254, 255]. Using Monte Carlo techniques, he studied the same kind of uncorrelated roughness as for the stripes: Gaussian distribution of thicknesses with integer mean L and ΔL constant for all L or $\Delta L = L/L_0$ [254] as well as noninteger mean L [255]. These studies were partly motivated by the observation that some film quantities depend on the growth condition, different growth mechanisms leading to different types of roughness. Reis studied the magnetic susceptibility, the specific heat and the total magnetization of films with different thicknesses. Especially, he showed that the simple equation (19) connecting the critical temperature of finite films with the bulk critical temperature does not hold for noninteger mean thicknesses L, as $T_c(L)$ shows a convex behaviour between two consecutive integer values of L [255]. He also studied the critical behaviour of rough films and thereby observed that the considered types of disorder are irrelevant: as for flat films, the critical exponents of the two-dimensional Ising model are recovered in rough thin films. Up to now only rough films with uncorrelated roughness have been studied. It would be very interesting to investigate the influence of spatial correlated roughness on the critical thin film behaviour as well.

The impact of additional regular structures, located at the surface, on the critical behaviour of Ising films is studied numerically in [90, 109]. The additional structures consist of one or two adjacent lines formed by adatoms as well as straight steps of unit height. One may introduce local couplings with different strengths, similar to what has been done in section 3.1 for the edges. For example, the strength of the bonds connecting two neighbouring adatoms in the defect line or the strength of the coupling between the adatoms and the underlying magnetic film may be varied. The main finding of [90] is that non-universal critical behaviour is encountered in Ising films with additional surface defects: the local magnetic critical exponents close to the defects depend continuously on the local couplings as well as on the layer thickness. Interestingly, the presence of an additional line is already enough to change the local critical exponent of a one-layer system by a large amount. Indeed, in the case where all the couplings have equal strength one obtains the value $\beta_l \approx 0.084 < 1/8 = \beta_{2D}$ for the critical exponent of the local order parameter [90].

It is worthwhile mentioning that related experiments on films with additional adatom lines have been published [274–276], even if there the lines of adatoms were not connected magnetically to the film. The magnetism of lines of four-dimensional adatoms on Ag surfaces has been the subject of some theoretical studies [277, 278]. The magnetic behaviour of thin films with large terraces has also been analysed experimentally [279].

Increasing the film thickness further, the semi-infinite system with surface imperfections is reached at the end. The following two typical scenarios must be distinguished: (i) for $J_s/J_b < r_{sp}$, bulk and surface order at the same temperature (ordinary transition), whereas (ii) for $J_s/J_b > r_{sp}$ the surface orders at a higher temperature than the bulk (surface transition). r_{sp} is the critical coupling ratio of the multicritical point, see section 2.1. Therefore, completely different behaviour of local quantities near the surface imperfections is expected in both cases when varying the number of layers L. Numerical simulations of non-perfect films are in complete agreement with this expectation [90]. For $J_s/J_b < r_{sp}$ the surface critical exponent $\beta_1 \approx 0.80$ is obtained in the limit $L \longrightarrow \infty$ everywhere on the surface, independently of any additional surface structure, as discussed already in section 4.1. In a film the local magnetization near the defect closely follows the local magnetization of the corresponding semi-infinite system for low temperatures. At temperatures where the correlation length is comparable with the thickness of the film a crossover from a regime with isotropic three-dimensional fluctuations to a regime dominated by two-dimensional critical fluctuations takes place. Increasing the film thickness the crossover temperature approaches the bulk critical temperature, yielding in the limit of the semi-infinite system, $L \longrightarrow \infty$, the value $\beta_l = \beta_1 \approx 0.80$ for the critical exponent of the local magnetization. Choosing $J_s/J_b > r_{sp}$, non-universal local critical behaviour close to the adchain is expected at the surface transition even in the limit $L \longrightarrow \infty$. This situation is indeed comparable to that of an edge at the surface transition, the edge corresponding to an extended defect line as discussed in section 3.2. The local magnetic critical exponents should therefore depend continuously on the local couplings at the additional line. This has been studied in [90] by examining the case $J_s = 2J_b$. The results obtained show that near an additional line β_l is affected both by the values of the local couplings and by the presence of additional bulk-like layers leading to non-universal local critical behaviour.

Further results have been obtained for systems with a straight step on top of film. At the ordinary transition, a straight step on top of a semi-infinite system does not change the local critical exponents [8]. In thin films the critical behaviour is however quite different [90, 109]. Introducing a straight step by adding half a layer of magnetic adatoms to the surface of the magnetic film one observes two sharp peaks in the specific heat [90, 109, 279], see figure 7, pointing to the existence of two different phase transitions. In fact, when considering a system with one half layer on top of a film one is dealing with a composite system displaying in the thermodynamic limit two distinct phase transitions at two different temperatures. Consider for simplicity the case of a single layer plus half a layer. One phase transition then takes place at the critical temperature of the two-dimensional Ising model, $k_B T_c(L = 1)/J_s = 2.269\ldots$ and one at the critical temperature of the double layer, $k_B T_c(L = 2)/J_s = 3.207(3)$. The value of the critical exponent of the step magnetization at the higher temperature phase transition is $1/2$, i.e. is identical to the value of the surface critical exponent of the two-dimensional Ising model.

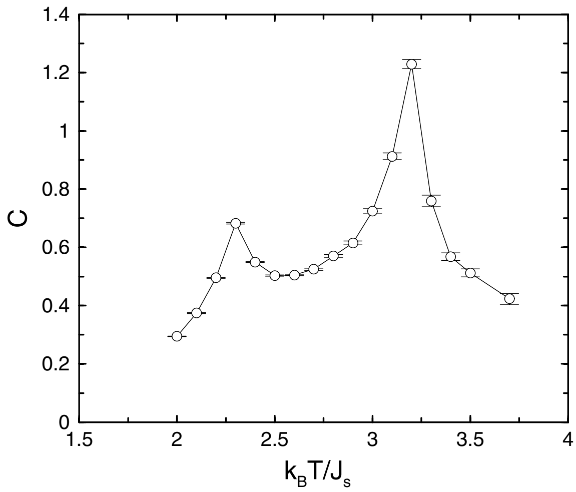

Figure 7. Specific heat of an Ising film with equal couplings consisting of one layer plus half a layer. Two distinct peaks are observed corresponding to two distinct phase transitions taking place in this composite system.

At the lower critical temperature the single semi-infinite layer then orders in the presence of ordered surface spins, the ordered double layer acting at that transition as a surface field. One is therefore dealing with the normal transition. The same scenario is expected to hold for finite films with an additional half layer with $T_c(L+1) > T_c(L)$, yielding at $T_c(L+1)$ the critical exponent $1/2$ near the step edge, in accordance with the numerical findings of [90] and [109]. Note that very recently [279], two sharp susceptibility peaks observed experimentally in thin films with large terraces have been interpreted as the signatures of two distinct phase transitions.

Thin films with an additional terrace covering half of the surface are only one example of composite systems displaying two distinct phase transitions. Further examples include two-dimensional Ising models with a defect column where the bonds differ on the two sides of the column [280], Ising quantum chains where couplings and transverse fields differ in the two half chains [281], or layered magnetic systems consisting of thin layers of coupled Ising spins with $S = 1/2$ and $S = 1$ [31]. In [282], wetting phenomena were studied in models consisting of two semi-infinite systems with unequal critical temperatures connected by a defect plane.

Finally, let us briefly mention that in the context of spin systems with continuous spin symmetry thin films with selected surface defects (amorphization of the surface layer [283] or steps [284]) have been considered in some cases, but no systematic study of the critical behaviour of this kind of systems has been done up to now.

5. Concluding remarks

The surface criticality has been the subject of intensive study in the last 30 years. Thereby a large variety of different methods (analytical, numerical and experimental) has been used, yielding a host of interesting results, as reviewed in this work. Critical phenomena at perfect surfaces are now in general well understood, at least when dealing with static critical quantities. This is not really the case for the dynamic critical behaviour at surfaces for which a coherent picture has not yet emerged. A major problem in this context is the total lack of experimental studies on surface dynamic properties at criticality. The situation is also not very satisfactory from the theoretical point of view, as only selected results on equilibrium and non-equilibrium surface dynamic behaviour at criticality have been published. Clearly, this is one of the most important aspects of surface criticality that warrants more attention in the future.

Wedge-shaped geometries, which can be viewed as generalizations of semi-infinite systems, have also been discussed in detail in this review. It is encouraging that the effect of curved surfaces on the local critical behaviour has been observed in simulations of liquid–vapour transitions near a weakly attractive surface. This may point to possible experimental systems where this kind of problem can be studied. There are indeed a vast number of theoretical predictions for this kind of geometry, and experimental investigations are therefore welcome.

In the last few years, the focus of research on the surface criticality has somehow shifted, as the main emphasis has been on more realistic surfaces. The facts that real surfaces are usually rough, displaying a variety of different surface defects, and that experimental physicists can create artificial structures on top of a surface directly lead to the question whether these quantities have an impact on local critical behaviour. We have presented a comprehensive overview of the field, thereby discussing in detail critical behaviour in semi-infinite systems with surface defects as well as in thin films with additional surface structures. Some common surface defects have been shown to be irrelevant for the surface critical behaviour at the ordinary transition. There are however some interesting exceptions, such as for example the case of self-affine rough surfaces. The situation is even more complex at the surface transition where in a three-dimensional system the critical fluctuations are of two-dimensional nature. Indeed, additional structures such as steps or lines of adatoms have been shown in numerical studies to lead to non-universal local critical behaviour where the values of the local critical exponents reflect the strengths of the coupling constants as well as the presence of the disordered bulk. It is worth noting that in thin films this kind of additional surface structure in general leads to non-universal critical behaviour.

It is obvious from our overview that a large number of recent studies of the effects of surface defects on local critical behaviour are either of purely numerical nature or are using rather crude approximations. This is especially the case when dealing with non-perfect surfaces at the surface transition. There is a need for more elaborate analytical approaches, and it is one of the intentions of this review to encourage further theoretical (and also experimental) investigations of critical phenomena at non-perfect surfaces.

Acknowledgments

It is a pleasure to thank all my collaborators who worked with me on various aspects of surface criticality: F Á Bagaméry, D Catrein, M-C Chung, F Iglói, M Kaulke, I Peschel, W Selke and L Turban. I am indebted to W Selke for introducing me to the field of surface critical behaviour and for many years of fruitful collaboration. I also thank H W Diehl, M Henkel and A Hüller for many inspiring discussions.

Note added in proof. After this work had been completed, Kimball *et al* [285] have published a paper where they studied the superfluid transition of ^{4}He in cells with various geometries, thereby measuring for the first time the edge specific heat at a phase transition.

References

[1] Binder K 1983 *Phase Transitions and Critical Phenomena* vol 8 (London: Academic) p 1
[2] Abraham A B 1986 *Phase Transitions and Critical Phenomena* vol 10 (London: Academic) p 1

[3] Diehl H W 1986 *Phase Transitions and Critical Phenomena* vol 10 (London: Academic) p 75
[4] Diehl H W 1997 *Int. J. Mod. Phys.* B **11** 3503
[5] Dosch H 1992 *Critical Phenomena at Surfaces and Interfaces* (Berlin: Springer)
[6] Fisher M E and Caginalp G 1977 *Commun. Math. Phys.* **56** 11
[7] Caginalp G and Fisher M E 1979 *Commun. Math. Phys.* **65** 247
[8] Pleimling M and Selke W 1998 *Eur. Phys. J.* B **1** 385
[9] Lubensky T C and Rubin M H 1975 *Phys. Rev.* B **12** 3885
[10] Nakanishi H and Fisher M E 1982 *Phys. Rev. Lett.* **49** 1565
[11] Mills D L 1971 *Phys. Rev.* B **3** 3887
[12] Binder K and Hohenberg P C 1972 *Phys. Rev.* B **6** 3461
[13] Binder K and Hohenberg P C 1974 *Phys. Rev.* B **9** 2194
[14] Burkhardt T W and Eisenriegler E 1977 *Phys. Rev.* B **16** 3213
[15] Lipowsky R and Wagner H 1981 *Z. Phys.* B **42** 355
[16] Binder K and Landau D P 1984 *Phys. Rev. Lett.* **52** 318
[17] Ruge C, Dunkelmann A and Wagner F 1992 *Phys. Rev. Lett.* **69** 2465
[18] Ruge C, Dunkelmann A, Wagner F and Wulf J 1993 *J. Stat. Phys.* **73** 293
[19] Au-Yang H 1973 *J. Math. Phys.* **14** 937
[20] Mermin N D and Wagner H 1966 *Phys. Rev. Lett.* **17** 1133
[21] Kosterlitz J M and Thouless D J 1973 *J. Phys. C: Solid State Phys.* **6** 1181
[22] Kosterlitz J M 1974 *J. Phys. C: Solid State Phys.* **7** 1046
[23] Fröhlich J and Pfister C E 1986 *Commun. Math. Phys.* **107** 337
[24] Landau D P, Panday R and Binder K 1989 *Phys. Rev.* B **39** 12302
[25] Peczak O and Landau D P 1991 *Phys. Rev.* B **43** 1048
[26] Diehl H W and Eisenriegler E 1984 *Phys. Rev.* B **30** 300
[27] Affleck I 2000 *J. Phys. A: Math. Gen.* **33** 6473
[28] Bakchich A and El Bouziani M 2001 *Phys. Rev.* B **63** 064408
[29] Iglói F and Carlon E 1999 *Phys. Rev.* B **59** 3783
[30] Benayad N and Dakhama A 1997 *Phys. Rev.* B **55** 12276
[31] Karevski D and Henkel M 1997 *Phys. Rev.* B **55** 6429
[32] Theumann A 1979 *Phys. Rev.* B **19** 6295
[33] De'Bell K and Essam J W 1980 *J. Phys. C: Solid State Phys.* **13** 4811
[34] Carton J P 1980 *J. Phys. (Paris)* **41** L175
[35] Christou A and Stinchcombe R B 1986 *J. Phys. A: Math. Gen.* **19** 757
[36] Diehl H W and Lam P M 1989 *Z. Phys.* B **74** 395
[37] Lipowsky R 1982 *Phys. Rev. Lett.* **49** 1575
[38] Lajzerowicz J 1981 *Ferroelectrics* **35** 219
[39] Turban L and Iglói F 2002 *Phys. Rev.* B **66** 014440
[40] Watson G M, Gibbs D, Lander G H, Gaulin B D, Berman L E, Matzke H and Ellis W 2000 *Phys. Rev.* B **61** 8966
[41] Lipowsky R 1982 *Z. Phys.* B **45** 229
[42] Dobrovolny C, Laanait L and Ruiz J 2004 *J. Stat. Phys.* **114** 1269
[43] Diehl H W and Shpot M 1994 *Phys. Rev. Lett.* **73** 3431
[44] Diehl H W and Shpot M 1998 *Nucl. Phys.* B **528** 595
[45] De'Bell K, Lookman T and Whittington S G 1990 *Phys. Rev.* A **41** 682
[46] Hegger R and Grassberger P 1994 *J. Phys. A: Math. Gen.* **27** 4069
[47] Landau D P and Binder K 1990 *Phys. Rev.* B **41** 4633
[48] Ruge C and Wagner F 1995 *Phys. Rev.* B **52** 4209
[49] Nightingale M P and Blöte H W J 1988 *Phys. Rev. Lett.* **60** 1562
[50] Krech M 2000 *Phys. Rev.* B **62** 6360
[51] Berche B 2003 *J. Phys. A: Math. Gen.* **36** 585
[52] Sigl L and Fenzl W 1986 *Phys. Rev. Lett.* **57** 2191
[53] Mailänder L, Dosch H, Peisl J and Johnson R L 1990 *Phys. Rev. Lett.* **64** 2527
[54] Burandt B, Press W and Haussühl S 1993 *Phys. Rev. Lett.* **71** 1188
[55] Alvarado S, Campagna M and Hopster H 1982 *Phys. Rev. Lett.* **48** 51
[56] Diehl H W and Dietrich S 1981 *Z. Phys.* B **42** 65
[57] Cardy J 1984 *Nucl. Phys.* B **240** 514
[58] Reš I and Straley J P 2000 *Phys. Rev.* B **61** 14425
[59] Deng Y and Blöte H W J 2003 *Phys. Rev.* E **67** 066116

[60] Diehl H W and Dietrich S 1981 *Phys. Rev.* B **24** 2878
[61] Rau C and Robert M 1987 *Phys. Rev. Lett.* **58** 2714
[62] Tang H, Weller D, Walker T G, Scott J C, Chappert C, Hopster H, Pang A W, Dessau D S and Pappas D P 1993 *Phys. Rev. Lett.* **71** 444
[63] Tober E D, Palomares F J, Ynzunza R X, Denecke R, Morais J, Wang Z, Bino G, Liesegang J, Hussain Z and Fadley C S 1998 *Phys. Rev. Lett.* **81** 2360
[64] Shick A B, Pickett W E and Fadley C S 2000 *Phys. Rev.* B **61** R9213
[65] Rau C 1983 *J. Magn. Magn. Mater.* **31–34** 874
[66] Rau C, Jin C and Roberts M 1988 *J. Appl. Phys.* **63** 3667
[67] Mamaev Y A, Petrov U V and Starovoitov S A 1987 *Sov. Phys.–Tech. Phys. Lett.* **13** 642
[68] Marynowski M, Franzen W, El-Batanouny M and Staemmler V 1999 *Phys. Rev.* B **60** 6053
[69] El-Batanouny M 2002 *J. Phys.: Condens. Matter* **14** 6281
[70] Murphy B M, Stettner J, Traving M, Sprung M, Grotkopp I, Müller M, Oglesby C S, Tolan M and Press W 2003 *Physica* B **336** 103
[71] Polak M, Rubinovich L and Deng J 1995 *Phys. Rev. Lett.* **74** 4059
[72] Arnold C S and Pappas D P 2000 *Phys. Rev. Lett.* **85** 5202
[73] Bray A J and Moore M A 1977 *J. Phys. A: Math. Gen.* **10** 1927
[74] Burkhardt T W and Diehl H W 1994 *Phys. Rev.* B **50** 3894
[75] Drewitz A, Leidl R, Burkhardt T W and Diehl H W 1997 *Phys. Rev. Lett.* **78** 1090
[76] Abraham D B and Upton P J 2000 *Phys. Rev. Lett.* **85** 2541
[77] Poulopoulos P and Baberschke K 1999 *J. Phys.: Condens. Matter* **11** 9495
[78] Ou J T, Wang F and Lin D L 1997 *Phys. Rev.* B **56** 2805
[79] Henkel M, Andrieu S, Bauer P and Piecuch M 1998 *Phys. Rev. Lett.* **80** 4783
[80] Saber A, Ainane A, Dujardin F, El Aouad N, Saber M and Stébé B 2000 *J. Phys.: Condens. Matter* **12** 43
[81] Zhang R and Wills R F 2001 *Phys. Rev. Lett.* **86** 2665
[82] Cabral Neta J, Ricardo de Sousa J and Plascak J A 2002 *Phys. Rev.* B **66** 064417
[83] Barber M N 1983 *Phase Transitions and Critical Phenomena* vol 8 (London: Academic) p 145
[84] Krech M and Dietrich S 1991 *Phys. Rev. Lett.* **66** 345
[85] Krech M and Dietrich S 1992 *Phys. Rev.* A **46** 1886
[86] Krech M and Dietrich S 1992 *Phys. Rev.* A **46** 1922
[87] Li Y and Baberschke K 1992 *Phys. Rev. Lett.* **68** 1208
[88] Nickel B, Donner W, Dosch H, Detlefs C and Grübel G 2000 *Phys. Rev. Lett.* **85** 134
[89] Schilbe P, Siebentritt S and Rieder K-H 1996 *Phys. Lett.* A **216** 20
[90] Chung M-C, Kaulke M, Peschel I, Pleimling M and Selke W 2000 *Eur. Phys. J.* B **18** 655
[91] Marqués M I and Gonzalo J A 2000 *Eur. Phys. J.* B **14** 317
[92] Moussa N and Bekhechi S 2003 *Physica* A **320** 435
[93] Schulz B and Baberschke K 1994 *Phys. Rev.* B **50** 13467
[94] Guo W, Shi L P and Lin D L 2000 *Phys. Rev.* B **62** 14259
[95] Halilov S V, Perlov A Y, Oppeneer P M, Yaresko A N and Antonov V N 1998 *Phys. Rev.* B **57** 9557
[96] Qiu Z Q, Pearson J and Bader S D 1994 *Phys. Rev.* B **49** 8797
[97] Huang F, Kief M T, Mankey G J and Willis R F 1994 *Phys. Rev.* B **49** 3962
[98] Popov A P and Pappas D P 2001 *Phys. Rev.* B **64** 184401
[99] Bak P 1982 *Rep. Prog. Phys.* **45** 587
[100] Selke W 1988 *Phys. Rep.* **170** 213
[101] Yeomans J M 1988 *Solid-State Phys.* **41** 151
[102] Selke W 1992 *Phase Transitions and Critical Phenomena* vol 15 (London: Academic) p 1
[103] Neubert B, Pleimling M and Siems R 1998 *Ferroelectrics* **208–209** 141
[104] Hornreich R M, Luban M and Shtrikman S 1975 *Phys. Rev. Lett.* **35** 1678
[105] Elliott R J 1961 *Phys. Rev.* **124** 346
[106] Fisher M E and Selke W 1980 *Phys. Rev. Lett.* **44** 1502
[107] Selke W and Duxbury P M 1984 *Z. Phys.* B **57** 49
[108] Selke W, Catrein D and Pleimling M 2000 *J. Phys. A: Math. Gen.* **33** L459
[109] Selke W, Pleimling M, Peschel I, Kaulke M, Chung M-C and Catrein D 2002 *J. Magn. Magn. Mater.* **240** 349
[110] Selke W, Pleimling M and Catrein D 2002 *Eur. Phys. J.* B **27** 321
[111] Mello V D, Chianca C V, Dantas A L and Carriço A S 2003 *Phys. Rev.* B **67** 012401
[112] Charnaja E V, Ktitorov S A and Pogorelova O S 2003 *Preprint* cond-mat/0303294
[113] Diehl H W 2002 *Acta Phys. Slovaca* **52** 271
[114] Gumbs G 1986 *Phys. Rev.* B **33** 6500

[115] Binder K and Frisch H L 1999 *Eur. Phys. J.* B **10** 71
[116] Frisch H L, Kimball J C and Binder K 2000 *J. Phys.: Condens. Matter* **12** 29
[117] Jacobs A E, Mukamel D and Allender D W 2001 *Phys. Rev.* E **63** 021704
[118] Pleimling M 2002 *Phys. Rev.* B **65** 184406
[119] Diehl H W, Rutkevich S and Gerwinski A 2003 *J. Phys. A: Math. Gen.* **36** L243
[120] Diehl H W, Gerwinski A and Rutkevich S 2003 *Phys. Rev.* B **68** 224428
[121] Garel T and Pfeuty P 1976 *J. Phys. C: Solid State Phys.* **9** L245
[122] Kumar P and Maki K 1976 *Phys. Rev.* B **13** 2011
[123] Dietrich S and Diehl H W 1983 *Z. Phys.* B **51** 343
[124] Kikuchi M and Okabe Y 1985 *Phys. Rev. Lett.* **55** 1220
[125] Riecke H, Dietrich S and Wagner H 1985 *Phys. Rev. Lett.* **55** 3010
[126] Xiong G M and Gong C D 1989 *J. Phys.: Condens. Matter* **1** 8673
[127] Xiong G M and Gong C D 1989 *Z. Phys.* B **74** 379
[128] Frank D and Dohm V 1989 *Phys. Rev. Lett.* **62** 1864
[129] Binder K and Frisch H L 1991 *Z. Phys.* B **84** 403
[130] Diehl H W and Janssen H K 1992 *Phys. Rev.* A **45** 7145
[131] Diehl H W 1994 *Phys. Rev.* B **49** 2846
[132] Wichmann F and Diehl H W 1995 *Z. Phys.* B **97** 251
[133] Ritschel U and Czerner P 1995 *Phys. Rev. Lett.* **75** 3882
[134] Majumdar S N and Sengupta A M 1996 *Phys. Rev. Lett.* **76** 2394
[135] Mukherji S 1999 *Eur. Phys. J.* B **8** 423
[136] Krech M, Karl H and Diehl H W 2001 *Physica* A **297** 64
[137] Diehl H W, Krech M and Karl H 2002 *Phys. Rev.* B **66** 024408
[138] Pleimling M and Iglói F 2004 *Phys. Rev. Lett.* at press (*Preprint* cond-mat/0312583)
[139] Hohenberg P C and Halperin B I 1977 *Rev. Mod. Phys.* **49** 435
[140] Janssen H K, Schaub B and Schmittmann B 1989 *Z. Phys.* B **73** 539
[141] Dietrich S and Wagner H 1985 *Z. Phys.* B **59** 35
[142] Dietrich S 1990 *Magnetic Properties of Low-Dimensional Systems II* (Berlin: Springer) p 150
[143] Dietrich S 1988 *Phase Transitions and Critical Phenomena* vol 12 (London: Academic) p 1
[144] Bonn D and Ross D 2001 *Rep. Prog. Phys.* **64** 1085
[145] Binder K, Landau D and Müller M 2003 *J. Stat. Phys.* **110** 1411
[146] Symanzik K 1981 *Nucl. Phys.* B **190** 1
[147] McAvity D M and Osborn H 1993 *Nucl. Phys.* B **406** 655
[148] Ritschel U and Czerner P 1996 *Phys. Rev. Lett.* **77** 3645
[149] Czerner P and Ritschel U 1997 *Int. J. Mod. Phys.* B **11** 2075
[150] Czerner P and Ritschel U 1997 *Physica* A **237** 240
[151] Ciach A and Ritschel U 1997 *Nucl. Phys.* B **489** 653
[152] Maciolek A, Ciach A and Drzewiński 1999 *Phys. Rev.* E **60** 2887
[153] Maciolek A, Evans R and Wilding N B 2003 *J. Chem. Phys.* **119** 8663
[154] Cho J-H J and Law B M 2001 *Phys. Rev. Lett.* **86** 2070
[155] Brézin E and Leibler S 1983 *Phys. Rev.* B **27** 594
[156] Ritschel U 1998 *Phys. Rev.* B **57** R693
[157] Krimmel S, Donner W, Nickel B, Dosch H, Sutter C and Grübel G 1997 *Phys. Rev. Lett.* **78** 3880
[158] Schmid F 1993 *Z. Phys.* B **91** 77
[159] Leidl R and Diehl H W 1998 *Phys. Rev.* B **57** 1908
[160] Cardy J 1983 *J. Phys. A: Math. Gen.* **16** 3617
[161] Iglói F, Peschel I and Turban L 1993 *Adv. Phys.* **42** 683
[162] Barber M N, Peschel I and Pearce P A 1984 *J. Stat. Phys.* **37** 497
[163] Peschel I 1985 *Phys. Lett.* A **110** 313
[164] Kaiser C and Peschel I 1989 *J. Stat. Phys.* **54** 567
[165] Davies B and Peschel I 1991 *J. Phys. A: Math. Gen.* **24** 1293
[166] Davies B and Peschel I 1997 *Ann. Phys., Lpz.* **6** 187
[167] Abraham D B and Latrémolière F 1994 *Phys. Rev.* E **50** R9
[168] Abraham D B and Latrémolière F 1995 *J. Stat. Phys.* **81** 539
[169] Abraham D B and Latrémolière F 1996 *Phys. Rev. Lett.* **76** 4813
[170] Guttmann A J and Torrie G M 1984 *J. Phys. A: Math. Gen.* **17** 3539
[171] Duplantier B and Saleur H 1986 *Phys. Rev. Lett.* **57** 3179
[172] Karevski D, Lajkó P and Turban L 1997 *J. Stat. Phys.* **86** 1153

[173] Peschel I, Turban L and Iglói F 1991 *J. Phys. A: Math. Gen.* **24** L1229
[174] Landau D P 1976 *Phys. Rev.* B **14** 255
[175] Merikoski J, Timonen J, Manninen M and Jena P 1991 *Phys. Rev. Lett.* **66** 938
[176] Aguilera-Granja F, Morán-López J L and Montejano-Carrizales J M 1995 *Surf. Sci.* **326** 150
[177] Saxena V K 1987 *J. Phys. A: Math. Gen.* **20** 6623
[178] Grassberger P 1992 *J. Phys. A: Math. Gen.* **25** 5867
[179] Gaunt D S and Colby S A 1990 *J. Stat. Phys.* **58** 539
[180] Wang Z G, Nemirovsky A M, Freed K F and Myers K R 1990 *J. Phys. A: Math. Gen.* **23** 2575
[181] Saxena V K 1987 *Phys. Rev.* B **35** 3612
[182] Larsson T A 1986 *J. Phys. A: Math. Gen.* **19** 1691
[183] Mon K K and Vallés J L 1989 *Phys. Rev.* B **40** 2419
[184] Lai P Y and Mon K K 1989 *J. Phys. A: Math. Gen.* **22** 5167
[185] Privman V 1988 *Phys. Rev.* B **38** 9261
[186] Lai P Y and Mon K K 1989 *Phys. Rev.* B **39** 12407
[187] Cardy J L and Peschel I 1988 *Nucl. Phys.* B **300** 377
[188] Kachkachi H and Garanin D A 2001 *Physica* A **300** 487
[189] Pleimling M and Selke W 1998 *Eur. Phys. J.* B **5** 805
[190] Pleimling M 2002 *Comput. Phys. Commun.* **147** 101
[191] Pleimling M and Selke W 1999 *Phys. Rev.* B **59** 65
[192] Pleimling M and Selke W 2000 *Phys. Rev.* E **61** 933
[193] Brovchenko I, Geiger A and Oleinikova A 2004 *Preprint* cond-mat/0402030
[194] Fisher M E and Ferdinand F E 1967 *Phys. Rev. Lett.* **19** 169
[195] Bariev R Z 1979 *Sov. Phys.–JETP* **50** 613
[196] McCoy B M and Perk J H H 1980 *Phys. Rev. Lett.* **44** 840
[197] Ko L F, Au-Yang H and Perk J H H 1985 *Phys. Rev. Lett.* **54** 1091
[198] Turban L 1985 *J. Phys. A: Math. Gen.* **18** L325
[199] Delfino G, Mussardo G and Simonetti P 1994 *Nucl. Phys.* B **432** 518
[200] Oshikawa M and Affleck I 1996 *Phys. Rev. Lett.* **77** 2604
[201] Simões C S and Drugowich de Felício J R 1998 *J. Phys. A: Math. Gen.* **31** 7265
[202] Szalma F and Iglói F 1999 *J. Stat. Phys.* **95** 795
[203] Henkel M and Patkós A 1988 *J. Phys. A: Math. Gen.* **21** L231
[204] Henkel M, Patkós A and Schlottmann M 1989 *Nucl. Phys.* B **314** 609
[205] Turban L 2003 Private communication
[206] Costa-Santos R 2003 *Phys. Rev.* B **68** 224423
[207] Fröjdh P, Howard M and Lauritsen K B 1998 *J. Phys. A: Math. Gen.* **31** 2311
[208] Janssen H K, Schaub B and Schmittmann B 1988 *Z. Phys.* B **72** 111
[209] Kaiser C and Turban L 1994 *J. Phys. A: Math. Gen.* **27** L579
[210] Kaiser C and Turban L 1995 *J. Phys. A: Math. Gen.* **28** 351
[211] Lauritsen K B, Fröjdh P and Howard M 1998 *Phys. Rev. Lett.* **81** 2104
[212] Howard M, Fröjdh P and Lauritsen K B 2000 *Phys. Rev.* E **61** 167
[213] Hanke A, Krech M, Schlesener F and Dietrich S 1999 *Phys. Rev.* E **60** 5163
[214] Hauge E H 1992 *Phys. Rev.* A **46** 4994
[215] Napiórkowski M, Koch W and Dietrich S 1992 *Phys. Rev.* A **45** 5760
[216] Rejmer K, Dietrich S and Napiórkowski M 1999 *Phys. Rev.* E **60** 4027
[217] Parry A O, Rascón C and Wood A J 1999 *Phys. Rev. Lett.* **83** 5535
[218] Parry A O, Rascón C and Wood A J 2000 *Phys. Rev. Lett.* **85** 345
[219] Parry A O, Wood A J and Rascón C 2000 *J. Phys.: Condens. Matter* **12** 7671
[220] Parry A O, Wood A J, Carlon E and Drzewiński A 2001 *Phys. Rev. Lett.* **87** 196103
[221] Parry A O, Wood A J and Rascón C 2001 *J. Phys.: Condens. Matter* **13** 4591
[222] Bednorz A and Napiórkowski M 2001 *Phys. Rev.* E **63** 031602
[223] Lipowski A 1998 *Phys. Rev.* E **58** R1
[224] Abraham D B and Maciolek A 2002 *Phys. Rev. Lett.* **89** 286101
[225] Albano E V, De Virgiliis A, Müller M and Binder K 2003 *J. Phys.: Condens. Matter* **15** 333
[226] Milchev A, Müller M, Binder K and Landau D P 2003 *Phys. Rev. Lett.* **90** 136101
[227] Diehl H W and Nüsser A 1990 *Z. Phys.* B **79** 69
[228] Benyoussef A, Boccara N and Saber M 1985 *J. Phys. C: Solid State Phys.* **18** 4275
[229] Saber M 1987 *J. Phys. C: Solid State Phys.* **20** 2749
[230] Dakhama A, Fahti A and Benayad N 2001 *Eur. Phys. J.* B **21** 393
[231] Kaneyoshi T 1988 *Phys. Status Solidi* b **150** 297

[232] Kaneyoshi T 1989 *Phys. Rev.* B **39** 557
[233] Kaneyoshi T 1991 *Introduction to Surface Magnetism* (Boca Raton, FL: CRC Press)
[234] Wang J-S, Selke W, Dotsenko Vl S and Andreichenko V B 1990 *Physica* A **164** 221
[235] Kaneyoshi T and Shin S 1998 *Physica* A **260** 455
[236] Mon K K and Nightingale M P 1988 *Phys. Rev.* B **37** 3815
[237] Durian D J and Franck C 1987 *Phys. Rev. Lett.* **59** 555
[238] Harris A B 1974 *J. Phys. C: Solid State Phys.* **7** 1671
[239] Da Silva L R, Tsallis C and Sarmento E F 1988 *Phys. Rev.* B **37** 7832
[240] Shalaev B N 1994 *Phys. Rep.* **237** 129
[241] Feldman D E and Vinokur V M 2002 *Phys. Rev. Lett.* **89** 227204
[242] Iglói F, Turban L and Berche B 1991 *J. Phys. A: Math. Gen.* **24** L1031
[243] Cardy J 1991 *J. Phys. A: Math. Gen.* **24** L1315
[244] De Martino A, Moriconi M and Mussardo G 1998 *Nucl. Phys.* B **509** 615
[245] Pleimling M, Bagaméry F Á, Turban L and Iglói F 2004 *Preprint* cond-mat/0402188
[246] Nattermann T and Villain J 1988 *Phase Transit.* **11** 5
[247] Eisenriegler E, Kremer K and Binder K 1982 *J. Chem. Phys.* **77** 6296
[248] Diehl H W and Nüsser A 1990 *Z. Phys.* B **79** 79
[249] Diehl H W 1998 *Eur. Phys. J.* B **1** 401
[250] Bengrine M, Benyoussef A, Ez-Zahraouy H and Mhirech F 1999 *Physica* A **268** 149
[251] Zhao D, Feng L, Huber D L and Lagally M G 2000 *Phys. Rev.* B **62** 11316
[252] Mokrani A and Vega A 2001 *Phys. Rev.* B **63** 094403
[253] Bahmad L, Benyoussef A and Ez-Zahraouy H 2002 *Physica* **303** 525
[254] Aarão Reis F D A 1998 *Phys. Rev.* B **58** 394
[255] Aarão Reis F D A 2000 *Phys. Rev.* B **62** 6565
[256] Hanke A and Kardar M 2001 *Phys. Rev. Lett.* **86** 4596
[257] Hanke A and Kardar M 2002 *Phys. Rev.* E **65** 046121
[258] Duplantier B 1998 *Phys. Rev. Lett.* **81** 5489
[259] Cardy J 1999 *J. Phys. A: Math. Gen.* **32** L177
[260] Hilhorst H J and van Leeuwen J M 1981 *Phys. Rev. Lett.* **47** 1188
[261] Harris A B and Lubensky T C 1974 *Phys. Rev. Lett.* **33** 1540
[262] Grinstein G and Luther A 1976 *Phys. Rev.* B **13** 1329
[263] Ohna K and Okabe Y 1992 *Phys. Rev.* B **46** 5917
[264] Usatenko Z, Shpot M and Hu C-K 2001 *Phys. Rev.* E **63** 056102
[265] Usatenko Z and Hu C-K 2002 *Phys. Rev.* E **65** 066103
[266] Usatenko Z and Hu C-K 2003 *Phys. Rev.* E **68** 066115
[267] Iglói F, Lajkó P, Selke W and Szalma F 1998 *J. Phys. A: Math. Gen.* **31** 2801
[268] Lajkó P and Iglói F 2000 *Phys. Rev.* E **61** 147
[269] Palágyi G, Chatelain C, Berche B and Iglói F 2000 *Eur. Phys. J.* B **13** 357
[270] Aarão Reis F D A 1997 *Phys. Rev.* B **55** 11084
[271] Aarão Reis F D A 1998 *Physica* A **257** 495
[272] Aarão Reis F D A 1998 *J. Phys. A: Math. Gen.* **31** 9105
[273] Aarão Reis F D A 2001 *Physica* A **291** 375
[274] Shen J, Skomski R, Klaua M, Jenniches H, Manoharan S S and Kirschner J 1997 *Phys. Rev.* B **56** 2340
[275] Shen J, Pierce J P, Plummer E W and Kirschner J 2003 *J. Phys.: Condens. Matter* **15** R1
[276] Skomski R 2003 *J. Phys.: Condens. Matter* **15** R841
[277] Bazhanov D I, Hergert W, Stepanyuk V S, Katsnelson A A, Rennert P, Kokko K and Demangeat C 2000 *Phys. Rev.* B **62** 6415
[278] Bellini V, Papanikolaou N, Zeller R and Dederichs P H 2001 *Phys. Rev.* B **64** 094403
[279] Andrieu S, Chatelain C, Lemine M, Berche B and Bauer P 2001 *Phys. Rev. Lett.* **86** 3883
[280] Bariev R Z, Malov O A and Barieva N A 1990 *Physica* A **169** 281
[281] Berche B and Turban L 1991 *J. Phys. A: Math. Gen.* **24** 245
[282] Iglói F and Indekeu J O 1990 *Phys. Rev.* B **41** 6836
[283] Hamedoun M, Bakrim H, Hourmatallah A and Benzakour N 2003 *Surf. Sci.* **539** 155
[284] Zhao D, Liu F, Huber D L and Lagally M G 2002 *J. Appl. Phys.* **91** 3150
[285] Kimball M O, Mooney K P and Gasparini F M 2004 *Phys. Rev. Lett.* **92** 115301